UNIVERSITÀ
DI PARMA

DIPARTIMENTO DI MEDICINA E CHIRURGIA

CORSO DI LAUREA IN

PSICOBIOLOGIA E NEUROSCIENZE COGNITIVE

DISTINCT VENTROLATERAL PREFRONTAL CORTEX SECTORS DIFFERENTLY ENCODE VISUAL STIMULI DEPENDING ON TASK RULES: AN ELECTROPHYSIOLOGICAL STUDY ON MACAQUE MONKEY

Relatore:
Chiar.mo Prof. LEONARDO FOGASSI

Correlatore:
Chiar.mo Prof. STEFANO ROZZI
Chiar.mo Prof. CLAUDIO BASILE

Laureando:

DARIO CEFARIELLO

ANNO ACCADEMICO 2022-2023

Abstract

This study investigates the distinct roles of ventrolateral prefrontal (VLPF) areas in processing visual information within different contexts. Single-neuron activity was recorded from monkeys performing a passive visual task and visuo-motor tasks involving object interaction. VLPF areas were subdivided based on connectivity, and neuronal responses to stimuli were analyzed. Caudal VLPF areas showed increased involvement in visual processing, particularly in their responses to faces and graspable objects. Differential modulation of neural activity was observed across conditions, with caudal areas showing stronger responses to action-related tasks. Area 45A displayed strong responses to visual stimuli, possibly encoding object features or task difficulty. Caudal area 12r demonstrated strong coding of object identity, while middle area 46v encoded behavioral outcomes. Caudal area 46v exhibited robust responses during stimulus presentation, possibly reflecting early motor planning. Middle area 12r was involved in pragmatic object coding. Rostral areas showed less involvement in the studied functions. Overall, distinct VLPF sectors exhibit specific roles in processing visual information and guiding behavior, highlighting their different functional contributions in cognitive tasks.

Index

1. Introduction

1.1 Prefrontal Cortex Phylogeny and Ontogeny

Cerebral cortical surface areas exhibit considerable variation across species, even within primates, as evident by the notable difference present between the average surface area per hemisphere amounting to 1,843 cm² for humans, 599 cm² for chimpanzees, 193 cm² for macaques, 9.6 cm² for marmosets (Van Essen et al, 2018). The evolutionary origin of non-allometric prefrontal enlargement is traced back to the root of great apes, indicating that selection for changes in executive cognitive functions characterized both great apes and human cortical organization (J.B.Smaers et al, 2017). This process, initiated approximately 15-19 million years ago, reached its pinnacle in humans, where the prefrontal cortex constitutes 30% of the total cortical surface.

This growth was accompanied by a phylogenetic differentiation of cortical segments which led to the development of several qualitatively and functionally unique regions (Carlén, 2017). Comparative histological studies of the frontal cortex and from other brain regions suggest that the internal organization and size of individual cortical areas are specialized among the hominoids - and it is this specialization and reorganization of specific areas that sets the various differences observed among species. An example of this specialization could be the relative volume of white matter underlying prefrontal association cortices, which is larger in humans than in great apes (Semendeferi, 1994, 2002).

These observations are further supported by the concept of neoteny, a factor proposed to play a role in human's CNS development by influencing its maturation rate (Gould S.J., 1977), as evidenced by humans' prolonged nervous and physical development relative to other primates; such extended development periods could allow for more extensive neural connections and therefore greater potential for cognitive complexity. Coherently with this hypothesis, Somel and colleagues (Somel et al., 2009) analyzed gene expression in the prefrontal cortices of both human and non-human primates throughout postnatal development, finding that humans exhibited a notable surplus of genes displaying neotenic expression. Furtherly corroborating these findings, neuroimaging studies in humans have repeatedly shown that prefrontal areas don't

reach full maturity until adolescence (Chugani et al., 1987; Sowell et al., 1999; Tomas Paus, 1999).
The considered data suggest that disparities in ontogenetic development timing within the PFC of human and non-human primates may contribute to existing differences in both sexual and cognitive domains.

1.1.2 Anatomy of the PFC

Human PFC is situated anteriorly within the cerebral hemispheres, positioned ahead of the premotor and motor cortices. These three areas collectively constitute the frontal lobe, with the prefrontal cortex occupying the largest portion of it (Goldman-Rakic, 1987; R. E. Passingham, 1993).
This region is characterized by a considerable amount of areas - as per Brodmann's organizational framework - that are both granular or dysgranular. This distinctive histological composition sets this region apart from other sectors of the frontal lobe which predominantly consist of agranular areas, including primary motor cortex (Brodmann area 4) as well as the secondary motor areas (Brodmann area 6, including the PMC and the supplementary and pre-supplementary motor areas, SMA and pre-SMA).
The PFC is characterized by two sulci originating from the precentral sulcus: the superior frontal sulcus, which separates the superior frontal gyrus from the middle one, and the inferior frontal sulcus, which divides the middle from the inferior.

Using classical cytoarchitectonic Brodmann parcellation and topographical criteria, the prefrontal cortex (PFC) can be divided into three principal subdivisions:

1. **Lateral Prefrontal Cortex (LPFC):** This subdivision can be further delineated into two parts — the dorsolateral Prefrontal Cortex (DLPFC), encompassing the lateral aspects of Brodmann areas 8 (including FEF), 9, 10, 11, and 46, and the Ventrolateral Prefrontal Cortex (VLPFC), which comprises Brodmann areas 44, 45 (Broca's area), and 47.
2. **Medial Prefrontal Cortex (MPFC):** This region includes Brodmann areas 12, 24, and 32, along with the medial components of areas 8, 9, 10, 11, and a section of the anterior cingulate cortex (Brodmann areas 32, 33, 24).

3. **Orbitofrontal Cortex (OFC):** Consisting of Brodmann areas 13 and 47, as well as the inferior portions of areas 10, 11, and 13.

These granular prefrontal regions exhibit systematic changes in laminar structure: based on their granularity, they can be further categorized into real granular cortices (homotypic or eulaminated), characterized by high amount of granularity and a thick IV layer, and dysgranular ones, characterized by a thin IV layer (Carlén, 2017).

Semendeferi and colleagues (Semendeferi K. et al., 2002) compared the relative size of the frontal cortices of several primate species, including all hominoids, using magnetic resonance imaging and found that human frontal cortices were not disproportionately large in comparison to those of the great apes; humans had the largest frontal cortex (which ranged from 238.8 cm^3 to 329.8 cm^3), while great apes' values ranged from 50.4 cm^3 (in a chimpanzee) to 111.6 cm^3 (in an orangutan); still, these sizes appear proportional when compared to the overall size of the entire brain. Among all the non-human primates considered in this study, great apes were the ones with the highest similarity to the human brain ratio (Table 1).

Table 1. The relative size of the frontal cortex.

	Brodmann (1909)[7]*	Blinkov & Glezer (1965)[8]*	Present study**
Human	36.3	32.8	37.7 (± 0.9)
Chimpanzee	30.5	22.1	35.4 (± 1.9)
Bonobo	NA	NA	34.7 (± 0.6)
Gorilla	NA	NA	35.0 and 36.9
Orangutan	NA	21.3	37.6 (± 1.1)
Gibbon	21.4	21.2	29.4 (± 1.8)
Macaque	NA	NA	30.6 (± 1.5)
Cebus	22.5	NA	29.6 and 31.5

*Table 1: Relative size of the frontal cortex, expressed in percentage of the size of the entire cortex (Semendeferi et al., 002).Surface of frontal cortex in % of surface of cortex of cerebral hemispheres. **Volume of frontal cortex in % of volume of cortex of cerebral hemispheres. NA, not available.*

One more point of resemblance among non-human and human primates can be found in the macaque, the most useful model for comparative anatomo-functional studies and widely utilized in neuroscientific research, in which the PFC shares analogous structural divisions to those documented in the human brain (Fuster, 1997; R. E. Passingham, 1993).

Petrides and Pandya (Petrides & Pandya, 1994, 1999, 2002) raised the question about direct comparability among human and macaque's PFC, observing that the majority

of anatomical and physiological investigations concerning the macaque prefrontal cortex in the last 50 years have relied on numerical architectural nomenclature methods devoid of any comparative analysis between the cytoarchitecture of the human and macaque PFC. These discrepancies pose a noteworthy challenge when comparing experimental findings derived from studies on non-human primates and humans, as the criteria for parcellating these areas in the two primate species are not always consistent. To address this issue, they suggested a PFC subdivision that allows direct comparison between the macaque and human prefrontal cortices (Fig. 1).

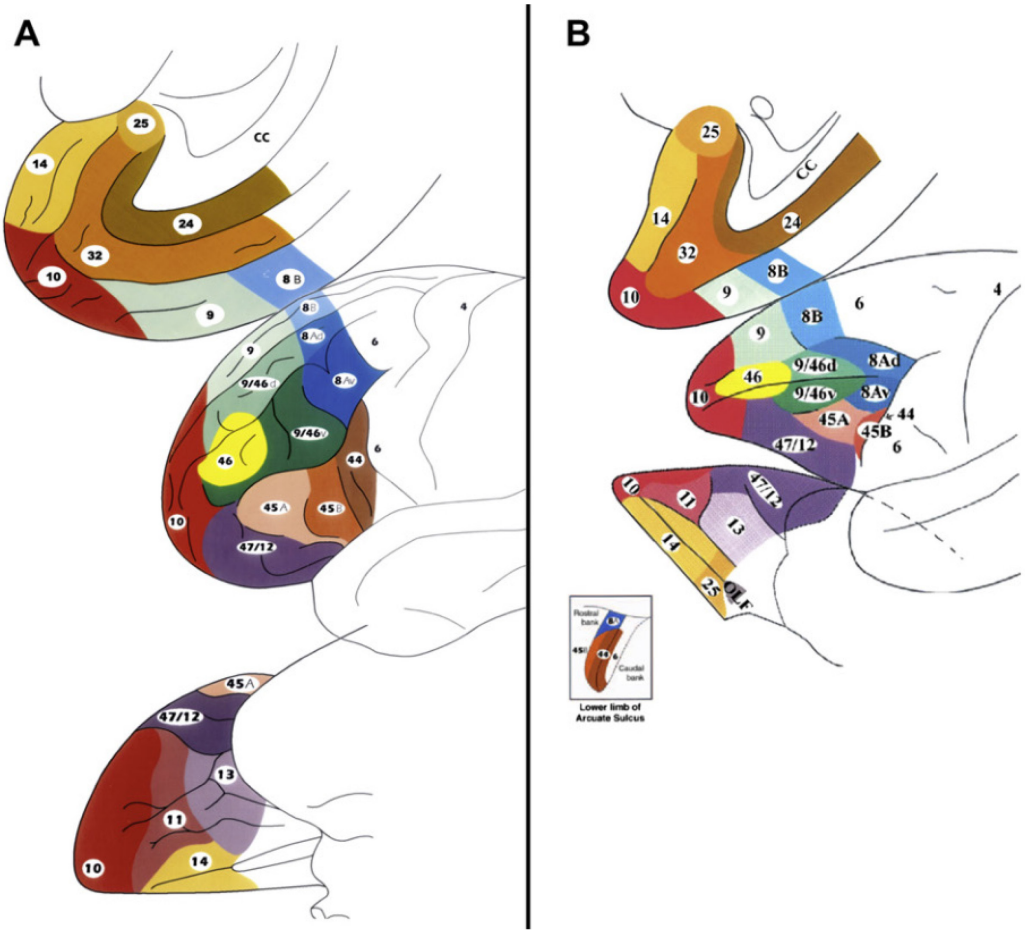

Figure 1: Cytoarchitectonic maps of the lateral, medial, and orbital surfaces of the frontal lobe of the human (A) and the macaque monkey (B) brains as parcellated by Petrides and Pandya (1994)

Petrides and Pandya also note that, despite some differences, the basic human and macaque PFC cytoarchitectural organization and pattern of anatomical connectivity has been preserved and is comparable, reinforcing the usefulness of macaque as an animal model in neurophysiological studies.

1.1.3 Anatomy of the macaque monkey ventrolateral PFC (VLPFC)

Petrides and Pandya compartmentalized monkey PFC into three principal divisions: orbital, medial and lateral, the latter of which develops last and most extensively and is comprised both in humans and non-humans primates of areas 12, 47, 45 and 46 in the ventral part and areas 5, 8b and 9 in the dorsal portion (Petrides & Pandya, 1999, 2002).

Using multi-architectonic and connectional techniques, the caudal VLPFC was furtherly subdivided by Luppino and collaborators (Gerbella et al., 2007) into several areas (Fig. 2):

• Three caudal regions, proximal to the arcuate sulcus: areas 8FEF, 8r, and 45B. • Three regions positioned on the ventral convexity: areas 45A, 12r, and 12l. • Two regions situated on the dorsal convexity: areas 8B and 9. • Two regions located within and surrounding the ventral and dorsal banks of the principal sulcus (PS): areas 46v and 46d, respectively.

• One region situated in the frontal pole: area 10.

They observed a gradual shift in the boundaries between areas, indicating the presence of intermediate points in this transition.

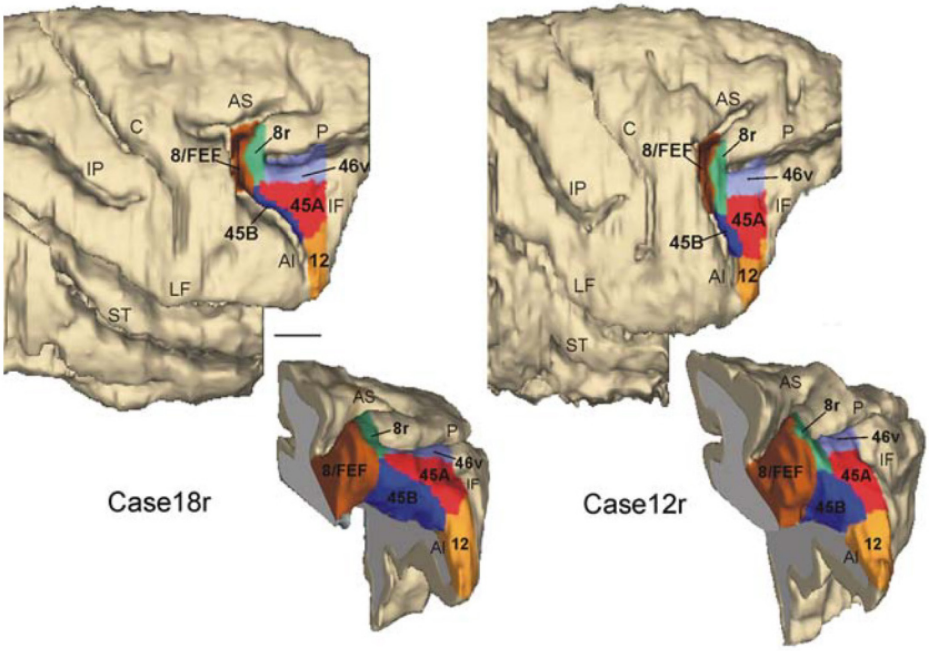

Figure 2:.3D reconstructions of the frontal lobe. For each case, the frontal lobe is shown from a dorso-lateral view (scale bar = 5 mm, for both reconstructions) and from a caudolateral view in which the anterior bank of the IAS was exposed with dissection of the 3D reconstruction along its fundus. (Gerbella et al., 2007).

1.1.3 Connectivity of the VLPFC

The lateral prefrontal cortex is organized in a dorsal and a ventral portion, divided by the Principal Sulcus (PS), and is directly and indirectly connected to widespread formations in the brain by the mediodorsal and orbito-ventral networks:

• The medio-dorsal network, encompassing the dorsolateral prefrontal cortex (DLPFC), receives inputs from multimodal areas situated in the temporal cortex or auditory regions of the superior temporal gyrus. Its involvement centers on the processing of spatial information. • The orbito-ventral network, which includes the ventrolateral prefrontal cortex (VLPFC), predominantly receives sensory inputs from visual, auditory, somato-sensory, gustatory, and olfactory areas, specializing in the processing of non-spatial information.

Moreover, these two networks exhibit extensive interconnections, enabling the LPFC to comprehensively integrate multiple sets of information on a large scale. This organizational framework plays a pivotal role in collecting, integrating, sorting, and modulating diverse sets of "data" processed in other regions of the brain (Petrides et

al., 2012; Petrides & Pandya, 2002; Preuss & Goldman-Rakic, 1989; Tanji & Hoshi, 2008).

Based on connectivity investigations (Borra et al., 2017; Gerbella et al., 2017), the LPFC has been subdivided into three vertically aligned strips, positioned in a caudo-rostral configuration. The most caudal strip primarily establishes connections with parietal regions (mainly LIP) and frontal areas (FEF and SEF), along with subcortical centers, specifically the intermediate and superficial layers of the superior colliculus. These connections are essential to the regulation of eye movements (Borra et al., 2015; Gerbella et al., 2010, 2013; Saleem et al., 2014).

At the same time, the rostral strip exhibits intra-prefrontal connections, encompassing the frontal pole and orbital prefrontal areas (Borra et al., 2011; Gerbella et al., 2013; Saleem et al., 2014). In contrast, the intermediate strip establishes connections with parietal and premotor areas, as well as subcortical structures engaged in the coordination of grasping and reaching movements (Borra et al., 2011, 2014; Gerbella et al., 2013, 2016; Saleem et al., 2014).

Area 12r, 46v and 46d - which are located in the intermediate strip - collectively contribute to the parieto-frontal object-grasping network. However, each of these areas exhibits specific characteristics in their connectivity patterns. Notably, Area 12r establishes connections with area F5, particularly its anterior subdivision F5a, and AIP. Area 12r is additionally connected to the secondary somatosensory area (S2) and the rostral part of the ventral bank of the superior temporal sulcus (STS), potentially corresponding to area LB2, which is active during the observation of hand grasping actions (Nelissen et al., 2011). Additional connections were observed in the central part of the insula. The adjacent area 46v displays a connectivity pattern similar to that of area 12r, establishing connections with areas F5a and AIP, along with SII and the insula. Moreover, it presents a strong connection with area PFG, and to a lesser extent with area F6, cingulate motor area 24, and the temporal lobe (Gerbella et al., 2013).

Area 46d manifests relatively robust connections with dorsal and mesial premotor areas F7 and F6, along with less pronounced connections with ventrorostral F2. Additional connections of 46d include the cingulate motor area 24 and parietal areas PG and V6A (Saleem et al., 2014).

It is to be noted that the connections with the temporal lobe increase ventrally in the LPFC- suggesting a stronger role of ventral prefrontal areas in processing of object's semantics and recognition.

1.1.4 Functions of the PFC

As delineated earlier, the prefrontal cortex constitutes a network of interconnected neocortical areas characterized by a distinctive yet overlapping pattern of connectivity with nearly all sensory neocortical and motor systems, as well as an extensive array of subcortical structures. This intricate network serves as an optimal foundation for producing the diverse spectrum of information required for complex behaviors displayed by both humans and non-humans primates (Miller, 2000).

The PFC, in particular, plays an essential role in executive functions, such as planning and temporal organization of actions on the basis of specific internal goals, in which the integration of multisensory information plays a pivotal role, involving various cognitive processes. These processes include the selection of appropriate behavioral responses, the accurate attribution of affective value based on social context, inhibitory control, attention decision-making, working memory, as well as emotional regulation and expression (Barbas et al., 2003; Gray et al., 2002; Tanji & Hoshi, 2008).

Involvement of VLPFC in the "lateral grasping network"

The traditional interpretation proposes that the execution of grasping actions necessitates a mechanism facilitating the conversion of sensory information into compatible motor acts or limb movements. This process involves specific parieto-premotor circuits (Rizzolatti & Luppino, 2001), including the inferior parietal lobule (IPL) and the rostral segment of the ventral premotor cortex (PMv), area F5. Together, these regions are considered the essential components of the "lateral grasping network".

Area F5 hosts three types of neurons: purely motor neurons, mirror neurons and canonical neurons. Purely motor neurons are activated, as the name suggests, during the execution of a motor act independently of the available visual information, thus either in light or in dark.

Mirror neurons activate when performing goal-directed actions, involving interaction between an effector (such as the hand or mouth) and an object, as well as when observing analogous actions being performed by others.

Conversely, canonical neurons simply respond to the visual observation of objects characterized by specific shapes, sizes, or orientations, even in the absence of manual actions (Fluet et al., 2010; Murata et al., 1997). This response has been interpreted as

indicative of the visuo-motor transformation process, which begins with the observation of the physical attributes of an object that are then used to determine the representation of the potential motor act suggested by these physical attributes, therefore allowing interaction with objects (Rizzolatti et al., 2014; Rizzolatti & Luppino, 2001).

Since the initial investigations of the monkey's parietal cortex, it has been established that a considerable number of neurons in the inferior parietal lobule (IPL) exhibit activation patterns during hand manipulation and grasping; they also appear to be associated with the visual guidance of reaching movements (Hyvarinen & Poranen, 1974; Mountcastle et al., 1975).

Located close to the IPL is the anterior intraparietal area (AIP), situated within the anterior region of the lateral bank of the macaque intraparietal sulcus. This area is recognized for its involvement in the grasping circuit (Murata et al., 2000; Sakata et al., 1995; Taira M. et al., 1990) as it is the parietal region that shares the most connection with F5. This area has been demonstrated to encompass neurons linked to hand movements, which can be classified into three groups: motor-dominant neurons, visual-dominant neurons, and visual-motor neurons (Taira M. et al., 1990).

- *Motor-dominant* neurons are active during grasping actions performed in both light and dark conditions, but not during simple observation of objects;
- *Visual-dominant* neurons responded during grasping in visible conditions and during simple object observation, but were completely silent during motor act execution in the dark (Murata et al., 2000; Sakata et al., 1995; Taira M. et al., 1990);

It’s also been proposed that, along with these three classes of neurons, IPL contains another neuronal category elicited during the visual presentation of hand actions of other individuals, modulating their activity in response to the observation of hand movements without the presence of an object (Baumann et al., 2009), suggesting the possibility of a pragmatic information encoding mechanism, which can be used to specify how to perform an action.

The simultaneous recording of AIP, F5 and F1 neurons corroborated the hypothesis that these regions contribute jointly to process information about an object during the execution of a reaching hand movement (Schaffelhofer & Scherberger, 2016).

The grasping network is comprised of many areas each with distinct roles:

• AIP specializes in processing visual information crucial for object grasping, such as shape, size and orientation.
• F5 supports the movement's planning and execution.
• F1 is responsible for motor execution, becoming active during hand movement.

Adjacent to AIP, in the IPL's cortical convexity, is found yet another parietal area integral to the grasping circuit: PFG. It hosts motor, somatosensory, visual and mirror neurons as well as neurons responsive to the sole object vision and hand actions directed at these objects (Borra et al., 2008; Ferrari et al., 2005; Hyvärinen, 1981). AIP and PFG establish dense interconnections, integrating one more parietal area - V6A, located in the most caudal portion of the superior parietal lobule - receiving information about the shape, location and distance of visual stimuli from dorsal visual pathway areas. Moreover, AIP receive informations from the ventral visual pathway areas such as IT regarding representations of object identity (Borra et al., 2008; Rizzolatti et al., 2006).

The capacity to choose and regulate suitable actions within a specific context, which is a fundamental aspect of organizing actions, depends on the functioning of the LPFC (Hoshi et al., 2000; Tanji & Hoshi, 2001).

The LPFC is diffusely connected to various regions, encompassing the parieto-premotor circuits as well as subcortical structures such as the basal ganglia and cerebellum (Tanji & Hoshi, 2008). These connections contribute to LPFC's engagement in various functions within its dorsal and ventral subdivisions:

- The dorsolateral prefrontal cortex (DLPFC) is associated with elevated executive functions such as behavioral planning, monitoring, manipulation, and integration of multiple pieces of information.
- The ventrolateral prefrontal cortex (VLPFC) participates in processes like information retrieval from memory and information selection (Fuster, 2001; Tanji & Hoshi, 2008).

The lateral prefrontal cortex doesn't solely hosts ventro-dorsal differentiations in its functional organization, but rostro-caudal as well (Koechlin et al., 2003; Nee & D'esposito, 2016; Riley et al., 2016). In Constantinidis and colleagues (Riley et al., 2016) study, monkeys were tasked with passively observing visual stimuli belonging to three categories: spatial, shape, and color. The only required behavior from the monkeys was to focus attention on the presented stimulus. The primary finding of this

study indicates a significant difference in spatial selectivity and information processing, with considerably higher levels observed in the dorsal regions compared to the ventral regions. This distinction was particularly evident in the spatial stimulus set employed, while shape selectivity and information did not exhibit differentiation between dorsal and ventral areas. The analysis of color differences showed only modest variations. This led to hypothesizing a functional differentiation between a more stimulus-category-selective posterior PFC and a more abstract-processing anterior PFC.
Numerous studies have shown that neurons active in oculomotor tasks are located more posteriorly (Boch & Goldberg, 1989; Satoe Ichihara-Takeda & Shintaro Funahashi, 2007), while, neurons involved in forelimb movement tend to be positioned more anteriorly, as observed in studies by Funahashi et al. (1993) and Hoshi et al. (1998), within the posterior two-thirds of the PFC.

The data presented indicate a modular arrangement within the VLPFC, wherein executive functions related to oculomotor behavior control are located more caudally while skeletomotor behavior functions are found in the more rostral regions. Consistent with this organization Simone and colleagues (Simone et al., 2015) demonstrates that neurons responding during reaching and grasping actions across various contexts are predominantly located within the intermediate sectors of areas 46v, 46d and 12r, which are all densely connected to premotor and parietal areas involved in the same category of actions.

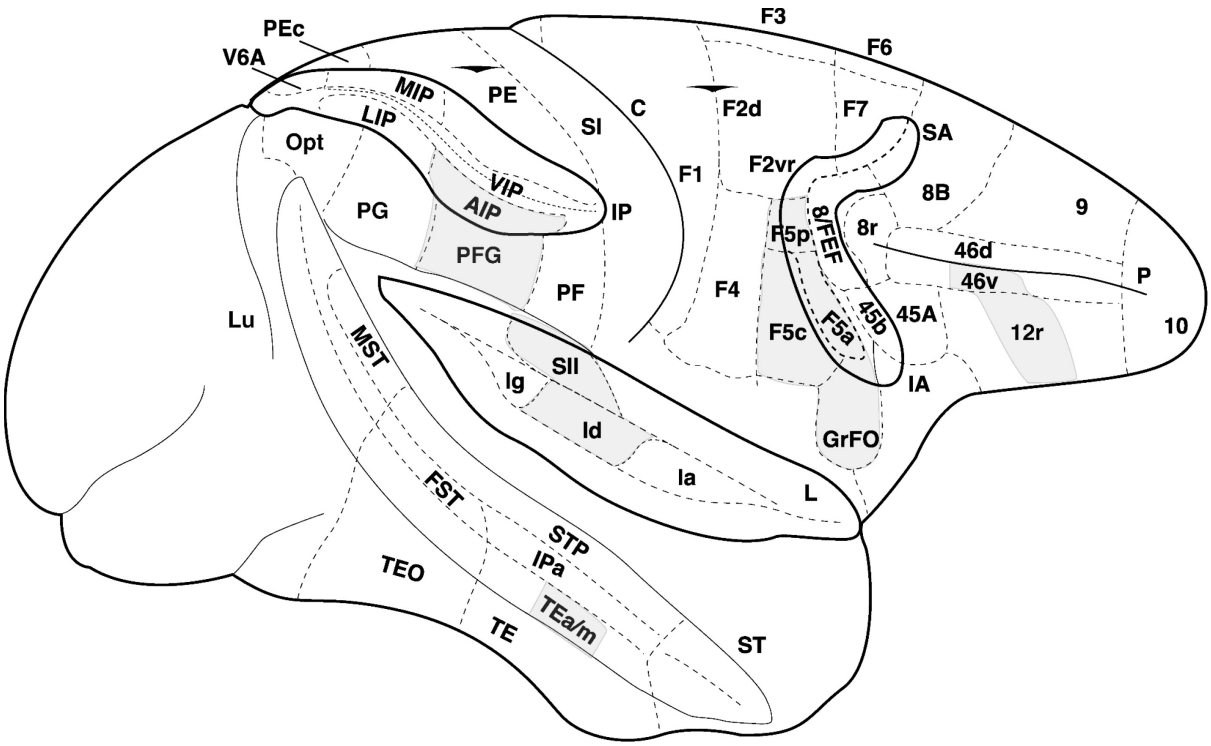

Figure 3: Schematic view of the lateral cortical surface of the macaque brain showing the areal subdivision of the frontal, parietal, insular and temporal cortex. Cortical areas/fields taking part in the lateral grasping network are highlighted in gray. The superior (SA) and inferior (IA) arcuate, intraparietal (IP), lateral (L) and superior temporal (ST) sulci are shown unfolded to display the location of cortical areas buried in their banks. C, Lu and P indicate the central, the lunate and the principal sulcus, respectively (Borra et al., 2017).

1.1.5 Connectional and functional specificity of the areas constituting the VLPFC

Area 12r is considered to be involved in working memory for objects and shapes (Wilson et al., 1993) as well as conditional learning based on object identity (R. E. Passingham, 1993; R.E. Passingham et al., 2000) and visual categorization (Freedman et al., 2002; Miller et al., 2002). This area exhibited a rostro-caudal gradient of connections (Borra et al., 2011; Gerbella et al., 2010; Saleem et al., 2014):

- The anterior segment, designated as 12r, primarily connects with prefrontal and orbitofrontal areas, along with the lower regions and upper bank of the STS.
- The middle segment shows connections with other prefrontal and orbitofrontal regions, as well as inferior and opercular parietal areas, ventral premotor hand-related areas and inferotemporal areas.
- The posterior region primarily connects to frontal oculomotor areas and inferotemporal regions. More specifically, the caudal 12r establishes connections with neighboring areas such as caudal 46v and 45A, as well as

areas 8r along with the most ventral subdivision of area 8-FEF (Gerbella et al., 2010).

Furthermore, caudal 12r also projects to superficial and intermediate layers of the superior colliculus (SC), to the reticular mesencephalic formation (RMF) and to the ooculomotor zones of the pontine nuclei (PnO) and of the caudate body (Borra et al., 2015). Regarding the functional aspect of these regions, electrophysiological investigations by Romanski and colleagues (Romanski, 2007; Romanski & Averbeck, 2009; Romanski L.M., 2004) show that a region composed by area 45A and a portion of the caudal area 12r contains neurons responsive to visual communication stimuli; this responsiveness likely stems from input to this area from higher-order multisensory anterior temporal regions. Additionally, fMRI data revealed an activation of a similar region during the observation of faces (Tsao & Livingstone, 2008) and other's actions (Nelissen K. et al., 2005).

In terms of motor output, specifically hand actions, especially those regarding an object, the brain relies on a network composed of AIP, SII, and F5 areas, with which area 12r plays a critical interacting role (Borra et al., 2017); this sector is, indeed, a site of integration of ventral visual stream information and sensorimotor hand-related information within the prefrontal cortex.

With these informations in mind, along with temporal connectivity data of area AIP, Cisek and Kalaska (Cisek & Kalaska, 2010) hypothesized that the ventral stream may have evolved to collect and elaborate visual information for action selection rather than for "pure" perception alone; coherently, the intermediate part of area 12r, which is densely connected to the ventral stream, is involved with retrieval, retention and elaboration of information on objects or hand-object interactions that could be directed towards the control of object-oriented hand actions. The presence of robust connectivity between AIP-F5-SII and orbitofrontal areas also suggests that the object's information being processed aren't only visuo-motor, but affective as well - meaning they reflect the "value" of objects in a more abstract manner (Schultz, 2000).

Caudal and middle areas 46v

Connectional studies paved the way for a subdivision of area 46 into a dorsal part (46d), which is most densely connected with superior and medial parietal and dorsal premotor areas (PMd - such as F7 and F2) and a ventral part (46v), mainly connected

to inferior and opercular parietal and ventral premotor areas (PMv) (Tanji & Hoshi, 2008).

Ensuing studies showed that connectivity in both sectors of area 46 is more complex than previously thought. The posterior region of area 46 is connected almost exclusively to frontal and parietal oculomotor areas; in particular, it's connected with prefrontal areas 8-FEF, 8r, 45b and the supplementary eye fields (SEF) as well as the caudal part of area 12r, dorsal premotor area and, within the parietal cortex, with area LIP.

More specifically, caudal 46v involves inferotemporal areas and areas FST and MT, while its dorsal part is mostly connected with parietal areas V6A and PGm and caudate cingulate areas 23 and 31 (Borra & Luppino, 2021).

Considering the density of connections between area 46, especially its most posterior subdivision, and the oculomotor regions - Lynch & Tian (Lynch & Tian, 2006) defined the caudal part of area 46 as "PFEF", prefrontal eye field.

This is due to the fact that numerous studies showed significant activation of neurons hosted within this region during tasks requiring oculomotor responses (Averbeck et al., 2006; Boch & Goldberg, 1989; Satoe Ichihara-Takeda & Shintaro Funahashi, 2007). Neurons in this region are also characterized by pre-saccadic activity (Funahashi et al., 1991), and by an encoding of visual Cue location or saccade direction in spatial working memory tasks (Funahashi & Takeda, 2002; Goldman-Rakic et al., 1990); these neurons are also active during delayed anti-saccade tasks (Funahashi et al., 1993) and modulated by the inactivation of area LIP during the performance of oculomotor delayed responses (Chafee & Goldman-Rakic, 2000) as well as during the sole execution of saccadic eye movements (Premereur et al., 2015) both voluntary and involuntary (such as during stimulus driven spatial attention shifting (Caspari et al., 2015). These data suggest a contributing role in control of spatial attention (Ibos et al., 2013; Thompson & Bichot, 2005), which is handled mostly by area 8-FEF. In particular, this region would be involved in the "on-line" maintenance of visuospatial information along with their utilization as mental representations of visuospatial coordinates within the spatial domain (Levy & Goldman-Rakic, 2000).

Area 46, especially the ventral part of its intermediate subdivision, is characterized by connections to parietal and frontal arm/hand-related areas: area F5a, SII and AIP (Gerbella et al., 2013). Coherently with these connectional data, along with informations regarding the strong connections with the intermediate region of area 12r,

middle 46v has a crucial role in selecting, monitoring and updating object-oriented hand actions based on behavioral goals, rules and working memory information on motor and object properties (Borra et al., 2017). Sensory and stimulus-related information processed in 12r could be then used in area 46v for intentional action selection (Tanji & Hoshi, 2008).

As a whole, this brain region appear to encode representations of consequences and development of actions, suggesting a role in governing goal-oriented sequential behavior, in encoding information representing multiple phases of behavioral actions (Saito et al., 2005; Shima et al., 2006; Saga et al., 2011).

Both middle 46v and middle 12r areas host multisensory neurons that appear to encode a behavioral decision independently from the sensory modality of the stimulus, while also coding contextual information for selecting and guiding object-oriented hand actions allowing the monkey to establish the most fitting response to the situation (Bruni et al., 2015).

Rostral portion of areas 12r and 46v

The rostral portions of areas 12r and 46v exhibit mostly and intrinsic prefrontal connectivity, with relatively weak extraprefrontal connections, mainly extending to the temporal and cingulate cortex. More specifically, the rostral part of area 12r is characterized by a dense connectivity with rostral prefrontal and orbitofrontal areas, contrasting with the relatively weak connectivity shared between the upper bank of the STS and cingulate area 24.

The rostral component of area 46v, compared to rostral 12r, shows a more extensive intra-prefrontal connectivity which involves not only ventrolateral and orbitofrontal areas, but also dorsolateral ones. At the same time, it shares similar extra-prefrontal connections to the rostral 12r, such as those directed towards the cingulate area 24. This pattern of connections suggests a role for both these components of area 12r and 46v in higher order aspects of the cognitive control of behavior.

Area 45A

What is today considered Area 45A (Petrides & Pandya, 1994), was actually considered as a part of a larger region, extended within Walker's area 12, that was shown to be active during object and faces encoding in working memory (Levy & GOldman-Rakic, 2000) or in conditional learning based on object characteristics (Passingham R.E. et al., 2000).

Subsequent studies lead to the consideration of this brain sector as its own area, based on connectional and functional properties which distinguished it from all the other VLPFC areas. From a connectional standpoint, tracer injections placed specifically in area $%A (Gerbella et al., 2010; Saleem et al., 2014) showed that this area is strongly connected to 45B, 8r, caudal 46, caudal 12r, SEF, the frontopolar area 10 and the rostral part of 46d. The dorsal compartment of 45A also shares connections with area 8-FEF.

Among all VLPFC areas, 45A is uniquely characterized by the fact that it's a target of temporal input from superior temporal gyrus' areas such as STP and rostral and caudal auditory parabelt areas. Connections to and from the parietal cortex, on the other hand, are rather weak.

Thalamic afferences from MDmf are relatively weak, differently from those from the central portion of the medial pulvinar which are, instead, robust (Contini et al., 2010).

Area 45A is a source of projections to the superior colliculus, encompassing both the intermediate and the most superficial layers while also sharing efferents fiber with other brainstem pre-oculomotor regions including the rostral MRF, also involving the parabigeminal nucleus and the ventrally adjacent PnO (Borra et al., 2015).

Many of the regions area 45A shares connections with are involved by some degree in oculomotor processes:

- dorso-medial and dorso-lateral portions of the pontine nuclei;
- oculomotor sectors of the caudate body and sub-thalamic nucleus;
- oculomotor zone of the caudate nucleus' tail;

Area 45A also shares strong afferent connections from the amygdala (Gerbella et al., 2014).

A series of studies conducted by Romanski and collaborators (Romanski L.M., 2004; Romanski, 2007; Romanski & Averbeck, 2009) showed that a region comprising of area 45A and a portion of area caudal 12r hosts neurons that show activation during

auditory, visual or combined auditory and visual communication stimuli - possibly integrating inputs from auditory-related temporal areas as well as higher-order multisensory area STP which contains neurons coding different types of biological motions (Oram & Perrett, 1994; Barraclough et al., 2005). Functional data suggest an involvement of area 45A in the control of communicative processes (Romanski, 2007; Romanski L.M., 2004; Sugihara et al., 2006), coherently with the proposed homology of this area with the corresponding language-related Broadman's area 44 and 45 in human brain (Petrides & Pandya, 2002), which together constitutes Broca's area.

The connectivity pattern that characterizes area 45A shows a strong connection with frontal and subcortical oculomotor centers. fMRI studies (Baker et al., 2006; Premereur et al., 2015)

showed that this area, like 8-FEF and 45B as well, activates during saccades execution, visual search tasks (Warak et al., 2010) and during attentional shifting in space (Caspari et al., 2015).

The aforementioned area STP shares dense afferences towards area 45A, and is involved in processing various forms of biological motion, including gaze direction and head direction, which may be relevant understanding where the conspecifics are fixating (Mistlin & Perrett, 1990; Ashbridge et al., 2000) and is involved in audiovisual communication signals integration (Barraclough et al., 2005; Chandrasekaran & Ghazanfar, 2009).

These data indicate that Area 45A along with caudal 12r are an integral component of the frontal oculomotor domain. Specifically, connections with area STP, the dorsal part of area 8-FEF and the amygdala could contribute in communication behavior of gaze direction, an important communicative signal in social interactions (Emery, 2000; Ghazanfar et al., 2006).

1.1.6 Action coding in the LPFC

Area middle 46 and 12r are part of an extended grasping network; to define the role of this and nearby regions, Simone and coworkers studied them (Simone et al., 2015), during a Go-NoGo task in which monkeys were required to either observe or execute grasping actions in different conditions, some of them based on abstract rules, others purely naturalistic. This study found that a sector, more or less recognizable as

the intermediate sectors of area 46, hosts the majority of neurons that are active during the execution of goal-directed reaching-grasping actions.

Some of these neurons were discharging more strongly when the object had to be grasped rather than simply observed. Finally, although some neurons showed a preference for a certain grip type, none of them showed a strong selectivity during object presentation. It was shown that movement-related neurons discharge during grasping in a variety of behavioral contexts (grasping under visual control, in no visibility conditions, memory-guided grasping and simple food grasping), showing that LPFC activity is not necessarily dependent on the learned association between instruction and motor output.

Coherently with results showing that the LPFC seems to process information about the visual context to generate goals by associating cues and goals (White & Wise, 1999;

Asaad et al., 2000; Miller, 2000; Wallis et al., 2001), many of the neurons analyzed in this study displayed a response during task epochs that anticipated movement execution. In fact, a high percentage of movement related neurons were also active 250 ms before the offset of the cue (Set epoch) and from the offset to the moment in which the hand had to release the grip (Go epoch), in agreement with studies describing LPFC cortex in movement planning (Funahashi et al., 1993; Quintana & Fuster, 1992, Averbeck et al., 2002; Quintana & Fuster 1992; Shima et al., 2006; Yamagata et al., 2012).

The different contextual conditions of the experimental paradigm (Motor condition in light and dark and the blocked motor condition) don’t seem to affect the neuron activation, as shown by population analyses, and could thus represent a type of preparation related to object “graspability” or the maintenance of action goal representation.

A following study expanded the population analysis (Rozzi et al., 2023) to the entire population of recorded neurons, rather than confine the analysis solely to a movement related neurons subpopulation, focusing specifically on the temporal dynamics of functionally identified populations of neurons during the exploitation of visuo-motor task based on foreseeing abstract rules (i.e Go/NoGo paradigm instructed by visual cues in which the monkey had to observe real objects and perform - in the action condition - or refrain to perform - in the inaction condition - object-oriented grasping actions).

This study revealed that the main factor influencing neural activation is the behavioral condition, Action/Inaction: the type of object being presented did not determine significant coding differences. The ratio of condition-dependent neurons is initially in favor of the Inaction condition during cue epoch, this proportion then shifts towards the Action condition during the object-presentation epoch. This result could be due to the fact that in the Inaction condition, in which the instruction is to withhold any action until reward delivery, the presentation of the instructing cue conveys sufficient information to correctly perform the task. Indeed, the subsequent object presentation and NoGo signal, although necessary for accomplishing the Inaction condition, are not relevant for the decision of which behavior to perform; on the other hand, in the Action condition the object that is presented is indeed significant as it determines the specific kind of action that has to be selected and performed. Thus, the Presentation of the object, in the Action condition, allows to progress from the general programming of behavioral goals (to act) to the specific program of the motor act to be executed. This could explain the shift in preference towards the Action condition that is observed in this epoch. In the whole population of neurons responding to Object Presentation as well as that of Condition-dependent Action neurons, the response is stronger in the Action condition not only in the Presentation epoch, but also from the go signal to the moment of object pulling. These findings are in line with the widely accepted idea that PFC neurons prospectively encode the behavioral output (Tanji & Hoshi, 2008). In addition, during the Action condition the population activity decreases abruptly during the holding phase, likely signaling goal achievement.

1.2 Aim of the study

Several functional studies contributed to the invalidation of the classical view according to which the LPFC could be considered as a single anatomical and functional region, showing that it is instead composed of relatively distinct areas and sectors. In particular, these studies evidenced a rostro-caudal inhomogeneity in the functional organization of the prefrontal lobe (Koechlin et al., 2003; Nee & D'esposito, 2016; Riley et al., 2016), which has been associated to a possible hierarchical functional organization progressing towards anterior areas (Badre & D'Esposito, 2009).

Moreover, neurons active during tasks requiring oculomotor responses are more caudally-located (Boch & Goldberg, 1989; Satoe Ichihara-Takeda & Shintaro Funahashi, 2007), while neurons that discharge during forelimb movement execution tend to be located more rostrally (Funahashi et al., 1993; Hoshi et al., 1998), within the posterior two-thirds of PFC. The LPFC functional subdivision here hypothesized is also supported by connectional data, which seem to suggest the presence of at least three vertical segments:

A posterior portion, primarily connected with the parietal and frontal areas and subcortical centers involved in oculomotor behavior control (Gerbella et al., 2010, 2013; Saleem et al., 2014; Borra et al., 2015), a more rostral portion connected with parietal and premotor areas and subcortical structures involved in skeletomotor behavior control (Borra et al., 2011, 2014; Gerbella et al., 2013,2016; Saleem et al., 2014) and, in the rostralmost part, a coding of abstract aspects of behavior would be implemented thanks to a dense network of intrinsic prefrontal connections (Borra et al., 2011; Gerbella et al., 2013; Saleem et al., 2014).

Rozzi and coworkers (Rozzi et al., 2021) previously analyzed the role of LPFC in the processing of visual information during the passive presentation of bidimensional stimuli or the presentation of tridimensional stimuli upon which the monkey was instructed to act or withhold an action, with no distinction regarding the neuronal populations recorded, showing that this region, studied as a whole, is characterized by an absence of any significant passive categorization of the various visual stimuli, but instead by a pictorial, passive description of the various stimuli potentially useful for behavior organization. In the same study a comparison was performed between the passive presentation of the three objects in a static visualization task and the presentation of those same stimuli in an action-oriented, motor task. The results showed that there was a higher response of neurons recorded in this region when the object is presented as a potential target of a motor action.

This study, as noted, considered the VLPF region as a whole, ignoring the various connectivity-based areas that have been identified in aforementioned studies (Gerbella et al., 2010, 2013,2016; Saleem et al., 2014; Borra et al., 2011, 2014,2015). This approach can help discerning the general functional role of the entire studied region but offers no insight about the possible differential distribution of the studied functional properties in the various recorded regions.

Based on these considerations, the present work is aimed at verifying:

1) whether the different VLPFC sectors are involved in visual stimuli categorization, even in the absence of a specific instruction.

2) whether neurons recorded in these sectors differently encode the presentation of pictures of graspable objects, occurring in a passive context, with respect to the presentation of the same, real, objects occurring in a context in which a hand-object interaction has to be performed or withheld, based on the current task rule.

To achieve these aims, we re-analysed the activity of previously studies neuronal populations which were recorded during the execution of different experimental tasks, in particular of a passive Visual task and a Visuo-motor Go/NoGo task, using single neuron and population analyses such as the dPCA and according to a connectional parcellation of the VLPFC based on previous neuroanatomical investigations (Gerbella et al., 2013; Borra et al. 2011).

2. Materials and Methods

The present study has been conducted on two female rhesus macaques (Macaca mulatta), Mk1 and Mk2, weighing ~4kg and aged, respectively, 4 and 5 years old. All experimental, housing and handling protocols as well as surgical and experimental procedures are compliant with European guidelines (2010/63/EU) and with Italian laws regarding the use of laboratory animals and their wellbeing and were approved by the Veterinarian Animal Care and Use Committee of the University of Parma (Prot. 78/12, 17/07/2012 and Prot. 91/OPBA/2015) and authorized by the Italian Health Ministry (D.M. 294/2012-C, 11/12/2012 and 48/2016-PR, 20/01/2016).

2.1 Training and surgical procedures

Before the recording phase, each monkey was gradually accustomed to interact with the experimenters, was taught how to sit comfortably in a primate chair and was made familiar with the experimental setup. At the end of the habituation phase, a head fixation system (Crist Instrument Co. Inc.), consisting of a titanium cylinder perpendicular to its “k-shaped” base, anchored to the cranial vault with titanium screws, was implanted. The head fixation system features three vertically aligned holes on its base, allowing it to be securely attached to the head positioner mounted on the primate chair.

This configuration minimizes the relative displacement between the brain and the recording electrode, thereby enhancing the stability of the neural recording and facilitating the precise evaluation of ocular position via an oculometer.

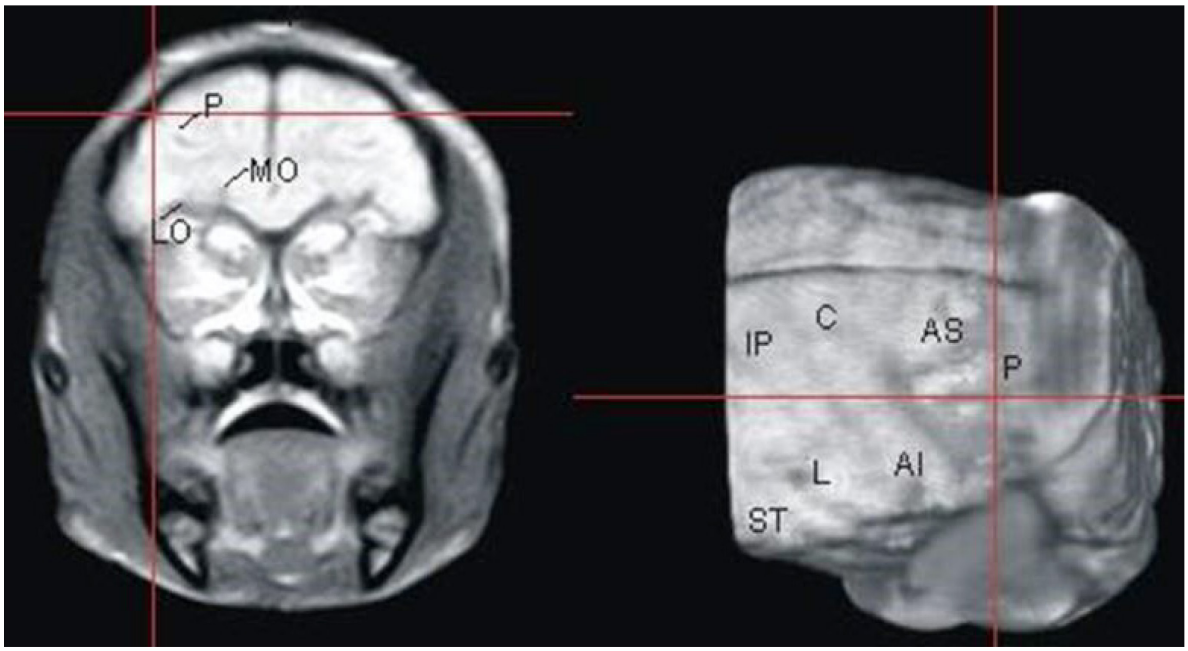

Figure 4: Images of the MRI used to plan the surgery. Left: coronal section passing through the VLPFC in a position corresponding to the coordinates of the middle area 46. Right: three-dimensional reconstruction of the brain showing the hemisphere in a dorso-lateral view tilted at 45° with respect to the middle-lateral plane after skull-stripping. The red crosses in the section and in 3D reconstruction indicates a location roughly corresponding the upper border of the recorded region. IA, inferior arcuate sulcus; IP, intraparietal sulcus; L, Lateral sulcus; LO, lateral orbital sulcus; MO, medial orbital sulcus; P, principal sulcus; SA, superior arcuate sulcus; ST, superior temporal sulcus. The images were obtained using the software MRI-cro on original scans captured through a 0.28T MR scan.

Each monkey was then trained to execute the task shown below, using the hand contralateral to the emisphere to be recorded. After training was completed, a second surgery was performed in which a bone flap was opened and a Cilux recording chamber (32 x 18 mm: Alpha Omega, Nazareth, Israel) was inserted at the level of the cortical region of interest in the left hemisphere, in order to allow access to the VLPFC.

These procedures were performed on the basis of a preliminary magnetic resonance imaging (0.28 T Paramed Medical Systems, Genoa, Italy; Fig. 4) of the brain of each monkey, performed in a veterinary clinic and under general anesthesia using ketamine (6.4 mg/kg) and medetomidine (0.08 mg/kg). This preliminary examination allowed the identification, in stereotaxic coordinates, of specific anatomical landmarks, used in the surgical site for the localization of the recording area.
During surgery, vital signs such as body temperature, heart rate, blood pressure, respiratory rate and depth were continuously monitored.

Dexamethasone, a potent anti-inflammatory and immunosuppressant (0.5 mg/kg, IM), mitigated surgical trauma and reduced post-operative complications. Additionally, broad-spectrum prophylactic antibiotics (e.g., ceftriaxone 80 mg/kg, IM) prevented potential bacterial infections, while analgesics (e.g., ketoprofen 5 mg/kg, IM) were employed to manage post-surgical pain.

Between recording sessions, the chamber before being sealed with the appropriate cap, was filled with a medicated solution (volume 16ml), consisting of agar dissolved in 8ml of physiological solution (4.6g/100ml), dexamethasone (0.5g / 100ml), rifampicin (0.06g / 100ml), gentamicin (0.02g / 100ml).

This combined approach aimed for synergistic effects. Antibiotics and dexamethasone worked together to control bacterial growth and minimize inflammation, creating a sterile environment. Solidified agar exerted pressure on the dura mater, hindering connective tissue proliferation.

This strategy addressed two key concerns:

1. Granulation tissue formation: This post-injury tissue can harbor bacteria. Suppressing it mitigated the risk of infection.
2. Electrode placement: Excessive connective tissue growth could impede accurate placement within the cortex. Solidified agar, by preventing its proliferation, facilitated precise electrode placement for reliable data collection.

2.2 Experimental Apparatus

During training and recording sessions, the monkey's head was restrained by fixating the implanted headpost to the head positioner of the primate chair. A cannula was placed near the monkey's mouth, allowing for fruit juice or water to be delivered acting as a positive reinforcement during training and experimental sessions. The primate chair was positioned in front of a horizontal shelf, placed at the same height of the animal's abdomen (80cm width and 60cm length) upon which was fixated, at a 6 cm distance circa, an aluminum cylinder connected to a contact-detection circuit on which the monkey had to position its hand at the beginning of each trial (starting position). A black box was positioned on the shelf , approximately 22 cm away from the animal. At the center of the box anterior side, there was a small door controlled by software, measuring 7 cm x 7 cm. Opening this door facilitated the presentation of one of three different objects contained within the box: a 1 cm diameter sphere, a horizontal cylinder (with a diameter of 1.5 cm and a length of 4 cm), and a cube (with sides measuring 2 cm each). Each object was categorized based on the type of grasping it afforded, determined by its dimensions and shape: a precision grip was suitable for the sphere, involving opposition between the thumb and index finger; a finger grip was appropriate for the cylinder, lacking thumb opposition; and a whole-handed grip with thumb opposition was suitable for the cube. Furthermore, each object was equipped with a contact-detection circuit, enabling precise measurement of hand-object contact during the motor task. Additionally, both on the box and the object, before and after the software-controlled door's opening, respectively, two laser dots of different colors (green and red) were projected. These dots served as fixation points and instructive cues simultaneously. In front of the monkey, positioned at a distance of 54 cm from its eyes, there was a computer monitor (with a resolution of 1680 x 1050 pixels) that allowed the presentation of visual stimuli (see below). The central point of the display was aligned with the monkey's eyes, while a phototransistor (Ates Medica Device s.r.l.) was placed in one corner, enabling accurate measurement of the timing of stimulus presentation on the screen. Above the monitor, a video camera sensitive to wavelengths in the visible spectrum and infrared, connected to a dedicated computer (integrated system I-SCAN ETL200 with a sampling frequency of 120Hz), allowed for tracking the position of the monkey's eye during the experimental tasks.

2.3 Eye position calibration

In order to monitor eye position during the various phases of the trials an ocular parameter calibration procedure was performed at the beginning of each training and recording session, programmed in LabView: on a 1680 x 1050 pixel resolution screen placed at a 54 cm distance from the monkey's eyes five red dots were presented, one at the time, in a randomized sequence, either at the center or in the 4 corners of the monitor. The monkey's task was to direct its gaze on each presented dot. This made it possible to register the pupil coordinates in the X and Y axes. The software, considering the distance between screen and monkey's eye along with the relative distances of the 4 dots presented on screen, transformed the signal acquired by the oculometer into angular coordinates that represented the direction in which the animal's eye had to move in order to fix that specific dot. This process defined a squared windows of 6° by 6° centered on the instructive stimuli (fixation point): the monkey had to keep its gaze within this window during the trials.

2.4 Experimental paradigm

The investigation into VLPFC neural properties involved conducting a visuo-motor task and two passive observation tasks featuring static and dynamic stimuli, respectively. These three tasks were executed in separate blocks. The presentation of the stimuli was arranged in a randomized fashion. To ensure robust and reliable statistical analyses, it was essential to achieve a minimum of 10 correct trials for each presented stimulus. A specially developed software managed the randomized presentation order of conditions and task events (such as cue on-off, door opening, reward emission, and output monitor), as well as the timing of task phases and eye positions. This information, along with analog and digital signals related to electrical recorded activity, was transmitted to an acquisition system. This system facilitated the precise correlation of neural activity with various experimental phases.

Visuo-motor task

The monkey performed a Go/No Go task consisting of a Motor (Action) and a Visual (Static) condition (Fig. 5). Each trial of both conditions commenced when the monkey placed its hand on the starting point. Subsequently, one of the instructing cues (red or green) was activated and projected onto the closed box door. In both conditions, the

monkey was required to maintain fixation within a 6°x6° degree square window centered on the instructing cue for a randomized interval of 500 to 1100 ms. If the monkey maintained fixation and did not move its hand from the starting position, the box door was then opened, and a light inside the box was simultaneously switched on, revealing one of the three objects.

During this period, the instructing cue continued to project onto the object, and the monkey was required to maintain fixation. After a randomized interval of 700ms to 1100ms, the instructing cue was turned off, serving as a Go/No Go signal. In the Motor/Action Condition, indicated by the green cue, the monkey was tasked with reaching for the object, grasping it with the appropriate grip, and holding it for a minimum of 600 ms. In the Visual/Inaction Condition, signaled by the red cue, the monkey had to maintain its gaze on the object for 600 ms. Upon successfully completing each correct trial, the monkey was rewarded with the release of a few drops of fruit juice.

A trial was discarded if any of the following errors occurred:

• The monkey failed to maintain fixation until the end of the trial.

• The monkey released its hand from the starting position prematurely, either throughout the trial in the visual condition or before the Go signal in the motor condition. • The monkey failed to reach for and grasp the object with the correct prehension, or it did not hold the object for the required duration.

Discarded trials were repeated at the end of the sequence to ensure the collection of at least 30 correct trials for each condition, corresponding to 10 correct trials for each object. The presentation order of both objects and conditions was randomized.

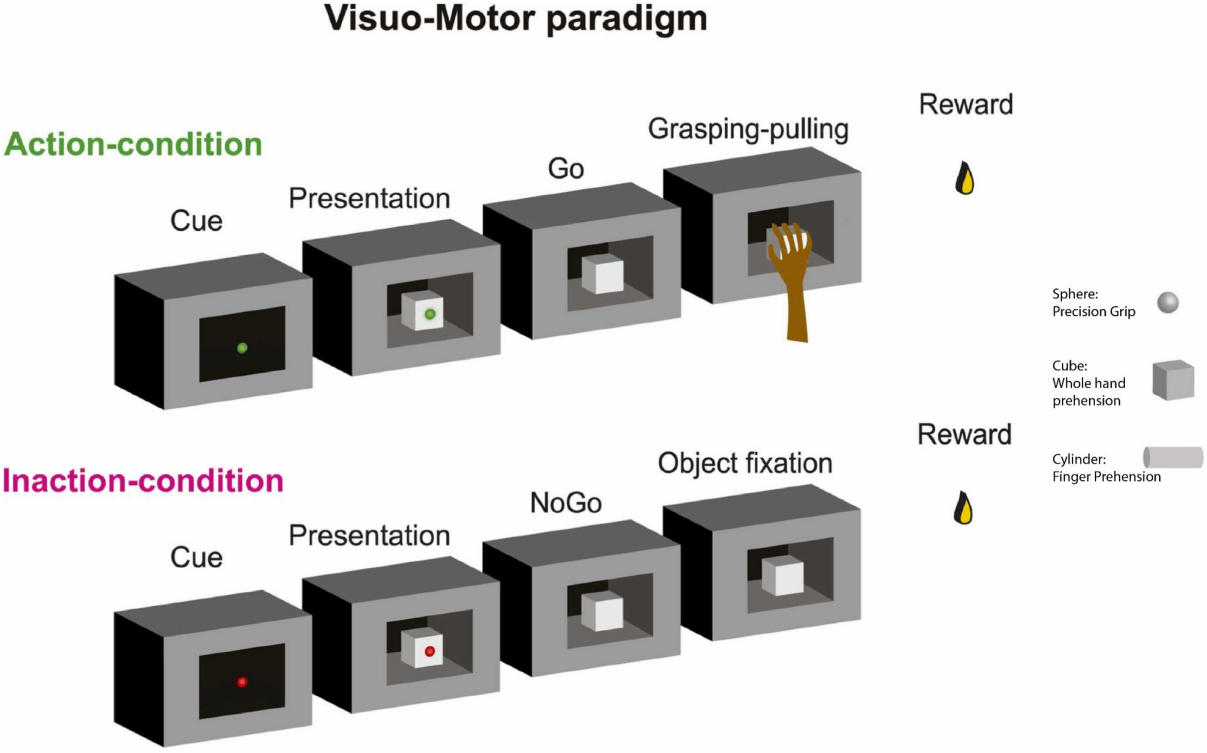

Fig. 5: Temporal sequence of events in the two conditions of the paradigm. The objects used in the task are depicted on the right. At the beginning of each trial, in both conditions, one of the two instructional lights was turned on. The green light instructed the monkey to perform a grasping movement on the presented object (motor condition); the red light instructed the monkey to fixate on the presented object and remain still (visual condition or Inaction condition).

2.4.2 Visual task with static stimuli

The task of static image observation involved the presentation of 12 two-dimensional stimuli (see below) that the monkey had to observe while keeping its gaze within a square fixation window (6° x 6°), centered on the fixation point and analogous to that described in the visuo-motor task. Figure 6A depicts the temporal sequence of events within each trial. Whenever the monkey kept its hand in the resting position, a laser projecting a red dot at the center of the monitor (fixation point) was activated. The monkey was required to fixate on this dot for a randomized period of time (500-900 ms) to ensure that its gaze remained within the fixation window during this interval: This led to the deactivation of the fixation point and the presentation of one of the images that the monkey had to observe for the entire presentation period, lasting 600 ms. Subsequently, the image disappeared, the fixation point was projected again onto the monitor for a randomized period of time (500-900 ms), and the monkey had to maintain fixation on it. If, at each phase of the task, the monkey maintained fixation within the window for at least 90% of the time and kept its hand still in the resting

position, the trial was considered correct, and the monkey was rewarded with the delivery of some drops of fruit juice. Incorrect trials were repeated at the end of the sequence to accumulate at least 10 correct trials for each stimulus. The presentation order of the stimuli was randomized. The presented images (Fig. 6B) belonged to four different semantic categories:

• Familiar graspable objects, not edible (two-dimensional images of objects used in the motor task): cylinder, cube, and sphere.

• Familiar graspable objects, edible (fruits): banana, apple, and peanut.

• Faces: monkey face, human face, and a drawing of a monkey face.

• Geometric but non-graspable objects: cabinet, computer screen, and clock.

All presented stimuli had a similar luminance profile and were composed of a uniform green background. Note that both graspable and non-graspable objects could evoke similar affordances (e.g., apple and cube: whole hand prehension; banana and cylinder: finger grip; sphere and peanut: precision grip).

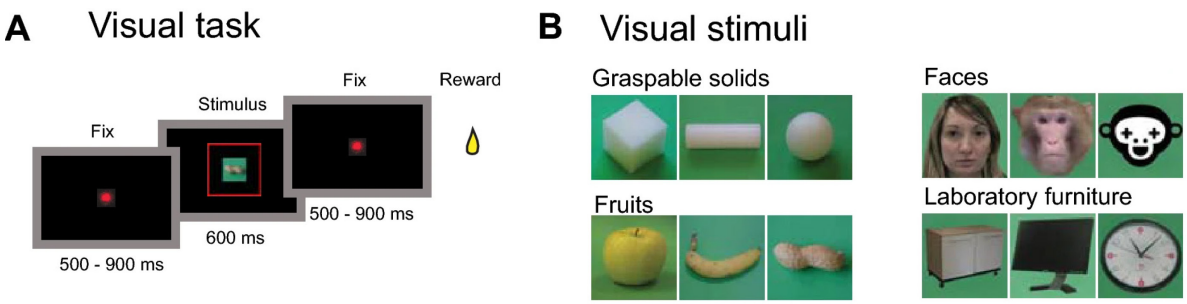

Fig. 6: Temporal sequence of events in the task of observing static images (A); stimuli presented in the visual task (B).

2.5 Recording and neuronal signal acquisition techniques

Neural recording has been performed using a multi-electrode system (Alpha Omega Eng., Nazareth, Israel) connected to a registration chamber. A micromanipulator (MT Microdriving; Fig 7) allowed for micrometric movements along the X, Y and Z axis. The micromanipulator supported eight glass-coated microelectrodes (diameter: 250 µm; impedance 0.5-1 MΩ), arranged in two rows of four electrodes each. The electrodes were positioned 2 mm apart to capture information from neurons spaced a few millimeters apart, allowing for comparison of their properties. Additionally, each electrode could be independently moved in depth thanks to a mechanical system controlled by an electronic motor block, operated by dedicated software (EPS or Electrode Position System, Alfa Omega). The recording parameters were defined by dedicated software (Multi Channel Processor MPC-Plus; Alpha Omega), which allowed filtering of neural activity from the electrodes (high-pass filter: 500 Hz, low-pass filter: 7.5 kHz, and notch filter), amplification of the signal (total amplification: 12000), and transmission to a computer (Alpha Lab, Alpha Omega) for acquisition and analysis. Using a graphical interface on the computer monitor, it was possible to observe the real-time output of multi-unit activity from each electrode. To identify and isolate individual unit waveforms from the overall signal of each electrode, an offline sorter (Plexon, Dallas TX, USA) was utilized.

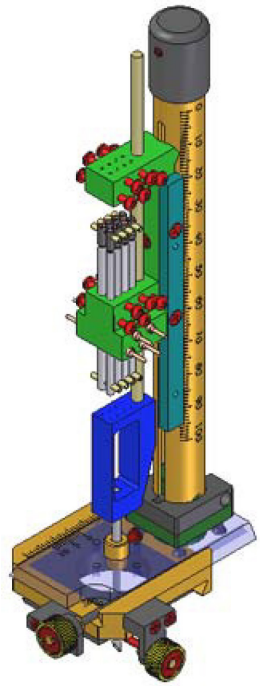

Fig. 7: Micro Driving Terminal, Alpha Omega Eng.

2.6 Preliminary mapping and PFC study

Before starting the neuronal data acquisition explorative penetrations have been performed to locate the precise position of LPFC and its borders.

This allowed the identification of both the cortical convexity region, where neural activity has been registered at a 2-3mm depth, and the regions located within the sulci, in which the electrode could record neural activity at depth exceeding 4mm.

Through this procedure, it was possible to delineate the course of the arcuate sulcus, which serves as the boundary between the premotor cortex and the prefrontal cortex. Further confirmation of this boundary was provided by analyzing the functional properties detected at each penetration. In particular, in the most rostral part of the sulcus, at the level of the prearcuate cortex, neural responses related to eye movements were observed, while the more caudal part, corresponding to the postarcuate cortex, exhibited neural responses related to the movement of the upper limbs, hands, and mouth.

In both exploratory penetrations and recording sessions, electrodes were initially inserted through the intact dura mater until the first neuronal events were detected. Subsequently, each electrode was progressively advanced in depth in successive steps of 250-500 μm each until reaching the boundary between gray and white matter. After a period of activity settling, neuronal activity recording was conducted during the execution of experimental paradigms and clinical trials. Once the initial acquisition phase was completed, in order to obtain a comprehensive and unbiased sampling of cortical activity, electrodes were further advanced to a depth of 500 μm for each subsequent acquisition, reaching a maximum depth of 2 mm in convexity areas and 4/5 mm in sulci.

2.7 Statistical analysis

Visual task

In the visual task, neural activity for at least 120 successful trials was recorded, 10 for each stimulus.

For the statistical analysis, two epochs were defined:

• *Baseline*: 500 ms preceding stimulus presentation, during which the monkey was looking at the fixation point;

• *Stimulus*: the first 500 ms of image presentation.

Single-neuron responses were statistically evaluated by means of a 2X12 ANOVA (Factors: Epochs, Stimuli, $p < 0.01$) followed by Newman-Keuls post hoc tests.

A neuron was considered visually responsive when the 2X12 ANOVA revealed:

1) A significant Main effect Epoch and/or
2) A significant Interaction effect, in which the Post-hoc test showed a significant difference between at least one stimulus epoch of one image and its baseline.

Visually responsive neurons were classified as selective when the 2X12 ANOVA revealed a significant Interaction effect and the post-hoc test showed a significant difference among the activity recorded in the stimulus epoch of one stimulus and that of (1) its baseline and (2) the stimulus epoch of at least another stimulus. Neurons were classified as unselective when the statistical test revealed a significant Main effect Epoch and/or a significant Interaction effect, and the post-hoc test did not show any difference among the activities recorded in the stimulus epoch of the 12 stimuli.

Comparison of neuron response between Visual and Visuo-Motor tasks

The recorded digital signals allowed the alignment of neural activity with specific behavioral events, in order to visualize neural activity as raster diagrams and histogram and perform a quantitative analysis.
During action and inaction conditions, neural activity has been recorded in at least 60 correct trials (30 for each condition, 10 for each object).
For the statistical analysis of the activity recorded in the Visuo-Motor task, 9 epochs have been defined, based on digital signals, as follows:
• *Baseline*: from 750ms to 250ms before the appearance of the instructive cue;
• *Pre-Cue*: 250ms before the instructive cue;
• *Cue:* 250ms after the instructive cue;
• *Pre-Presentation*: 500ms before the opening of the box's door;
• *Presentation*: Object presentation, 500ms after the opening of the door;
• *Set*: 250ms before the instructive cue's offset;
• *Go/NoGo*: from the instructive cue offset to the release of the hand from the starting position (action condition) or 250 ms after the deactivation of the instructional cue (inaction condition).
• *Grasp-hold/Fix*; from 250ms before to 250ms after the beginning of the grasping motion (Action condition) or from 250ms to 500ms after the instructive cue's offset (Inaction condition).
• *Reward*: within the following 500 ms after reward delivery.

Single-neuron responses underwent statistical analysis using a 9x2 ANOVA (Factors: Epoch, Condition, $p < 0.01$), followed by Newman–Keuls post hoc tests.

Comparison between the Visual and Visuo-Motor tasks was conducted on neurons identified as visually responsive in at least one task and whose neural activity was recorded in 90 successful trials—10 for each stimulus (Cube, Cylinder, and Sphere) in each condition (Visual, Action, and Inaction). Statistical analysis involved a 3x3 ANOVA (Factors: Conditions, Stimuli, $p < 0.01$), followed by Newman-Keuls post hoc tests.

Since the Visual and Visuo-Motor tasks were acquired in different blocks, to ensure that baseline activity was not changed across tasks, we compared the activity of each neuron during the period preceding the stimuli presentation of both tasks. To this aim we conducted a t-test between the baseline epochs of the Visual task and the pre-presentation epoch of the Inaction condition of the Visuo-Motor task. Note that in these two epochs the monkey had to keep fixation on the same red fixation point and was not required to program any movement. We discarded all neurons showing a significant difference between these two epochs.

2.7.1 Construction of the functional maps

The functional maps that we will show in this work have been designed on a cartesian plane defined by the coordinates identified during the penetrations. In these maps each recorded coordinate is represented by a hollow circle; the first two maps, one for each monkey, show all the coordinates in which at least one neuron has been recorded. The second maps depicts the proportion of presentation-related neurons compared to the total number of neurons recorded at each site; the last pair of maps depicts the percentage of category selective and non-selective neurons compared to the number of presentation-related neurons recorded in each site.
In these maps the size of the dots represents the percentage of presentation-related and category selective and non-selective neurons.

2.7.2 Histology, reconstruction of the recorded area and anatomo-functional comparison

Prior to sacrificing the animals, electrolytic lesions were conducted at predetermined coordinates within the recorded region using 10-μA cathodic pulses every 10 seconds.

Following a week-long interval, each animal underwent anesthesia with ketamine hydrochloride (15 mg/kg i.m.) followed by an intravenous lethal injection of pentobarbital sodium. Subsequently, they were perfused via the left cardiac ventricle with buffered saline, followed by fixative. The brain was then extracted from the skull, photographed, frozen, and sectioned coronally. Every second and fifth section (60 μm thick) from a series of five was stained using the Nissl method. The locations of penetrations were reconstructed using electrolytic lesions, stereotaxic coordinates, penetration depths, and functional properties. Specifically, penetrations exceeding 3000 μm were utilized to localize the principal sulcus (PS) and, in the caudal region of the recorded area, the inferior limb of the arcuate sulcus (IAS).

Subsequently, the location and extent of various ventrolateral prefrontal cortex (VLPFC) areas were determined based on their connectional properties, using existing literature maps (Gerbella et al., 2010; 2013; Borra et al., 2011) (Fig. 8). These maps define the extension of each VLPFC area based on the connectivity patterns observed in tracer injection sites. Specifically, four areas (areas 8, 45B, 45A, and caudal 12r) demonstrating oculotomor connectivity were identified in the caudal VLPFC; two areas with skeletomotor connectional features were located in the intermediate VLPFC (middle areas 12r and 46v); finally, two more rostrally situated areas (rostral areas 12r and 46v) were considered as a single entity due to their strong intra-prefrontal connectivity.

To map these areas in each recorded monkey, the connectivity maps were overlaid onto the histological reconstructions of each animal using a nonlinear transformation procedure. Various anatomical references, such as sulcal positions, served as anchor points for this process. The resulting connectivity map for each monkey was then superimposed onto their own functional maps, utilizing sulci and electrolytic lesions as reference points, enabling the attribution of each penetration to a specific anatomical sector. Areas 45B and 8 were excluded from the present study due to the small sample size of neurons recorded in each area.

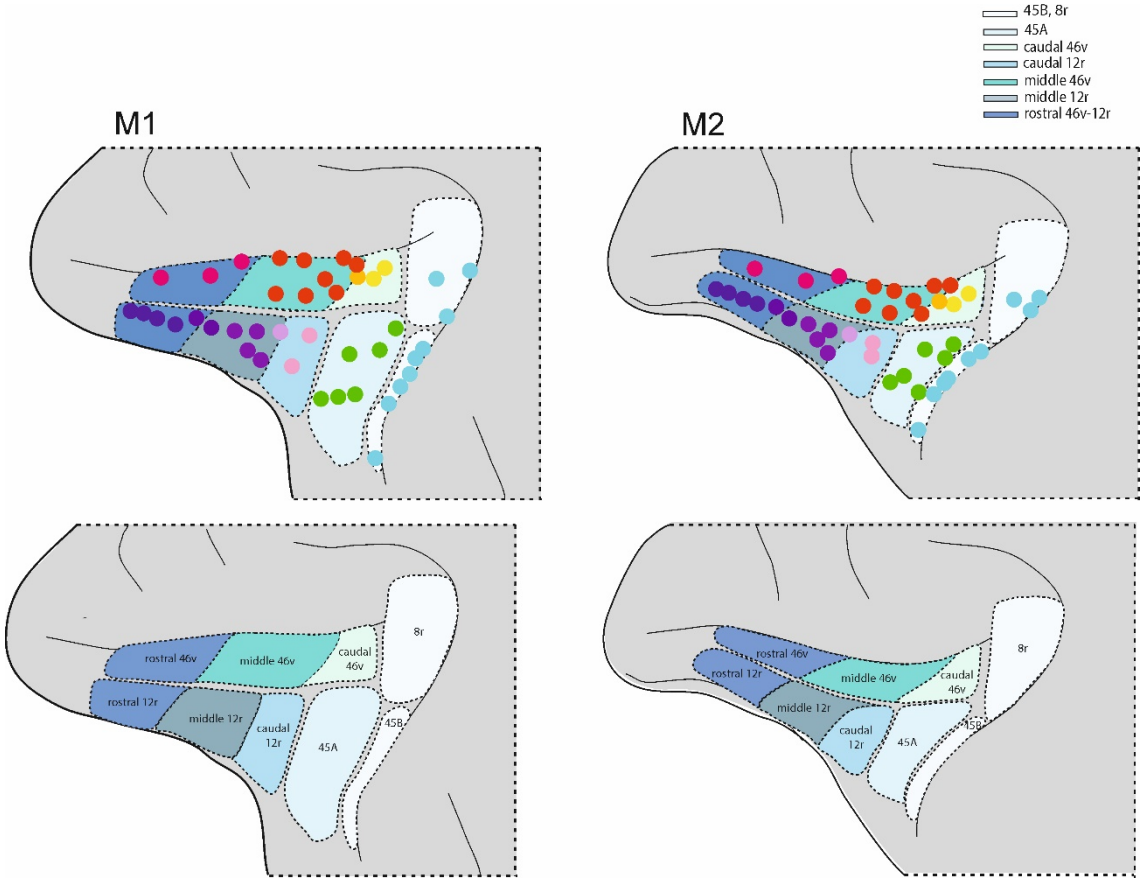

Fig. 8: Above, two-dimensional maps depicting the anatomical localization of the tracer injection sites having different connectivity patterns; injection sites referred to the same area are represented by dots of the same colour. Below, two-dimensional maps showing the different sectors recorded in M1 and M2.

2.7.3 Population analysis

To characterize the time course and the discharge rate of the different VLPF neuronal populations during the presentation phase of the Action and Inaction condition, in the visuomotor task, and of the Visual condition in the visual task, the neuronal activity of the populations of neurons responding in the visual or visuo-motor task (see Methods for the criteria of selection), recorded in each considered VLPF

sector, was aligned with the event of stimulus presentation on each task. For the visual task, we selected only those trials in which Graspable objects (i.e. the 2D versions of the objects presented in the Visuo-motor task) were presented. The mean single neuron activity over trials, in term of firing rate, was calculated for each 20 ms bin in the two conditions. The average activity in the “pre presentation period”, corresponding to 500 ms before stimulus presentation, was then subtracted from the mean single neuron activity over trials for each bin. Thus, in this analysis, 0 represents baseline activity. The net average discharge frequency of each neuron was used for subsequent statistical analysis. A one-way ANOVAs (factor: Condition, $p<0.01$, followed by post hoc Newman-Keuls) was performed in order to evaluate condition selectivity in the various areas during the Presentation epoch.

2.7.4 Demixed Principal Component Analysis

The demixed principal component analysis (dPCA) is a data-simplification method which allowed us to evaluate how the analyzed factors are encoded, in the presentation phase of the Visual task or by the different neuronal population of task-related neurons per area, considering together the data obtained from the two monkeys, during task unfolding (freely available code is provided by Kobak and coworkers, Kobak et al., 2016; http://githhub.com/machenslab/dPCA). In particular, we used this analysis focusing first on the Presentation phase of the visual task, and considering the category of presented stimuli (Graspable objects vs Food vs Faces vs Furniture) as our factor of interest, and then on the comparison between the Presentation phases of the Visual and Visuo-motor task, using Condition (Action, Inaction or Visual) and Object (Cube vs Cylinder vs Sphere) as our factors of interest. Note that, for the Visual task, we considered only the “Graspable objects” trials, as described above in the “Population analysis” section.

Besides reducing the dimensionality of dataset, dPCA uses information related to specific factors (Condition, Object or Category) to calculate the percentage of variance explained by the identified factors of the task. In addition, this analysis allows to identify components unrelated to the chosen factors, reflecting the dynamic changes of the population activity in time, which are similar for all factors. The toolbox uses a linear classifier (stratified Monte Carlo leave-group-out cross validation) to evaluate at which time points the given task elements belonging to a factor (i.e. Action vs. Inaction vs

Visual; Cube vs Cylinder vs Sphere; Graspable objects vs Food vs Faces vs Furniture) are significantly different from each other (see below).

For both the analysis of the Visual task and the comparison between Visual and Visuo-motor task, we first aligned the neural activity with the stimulus presentation, considering a period of 500 ms following stimulus appearance

Then, we classified the activity of task related neurons according to the possible types of trial (i.e., the four categories or the combination of the three conditions and the three types of objects), and calculated trial-by-trial the averaged 20-ms bins firing rate. The result was smoothed with a Gaussian-weighted moving average filter with a window of six 20 ms bins.

Starting from this dataset, we calculated the first 30 principal components. The number of repetitions used for optimal lambda calculation was 10, the number of iterations for cross-validation was 100, and the number of shuffles used to compute the Monte Carlo chance distribution was set to 100. Finally, we plotted the time course of the two largest demixed principal components for which variance was mainly attributable to the Condition and the Object factors as well as to other possible factors unrelated to them. We considered a statistical separation of the curves when the actual classification accuracy was at least 3 standard deviations above the mean chance accuracy, obtained after 100 shuffled decodings, in at least 5 consecutive 20 ms bins.

3. Results

3.1. Distribution of penetration sites and presentation-related neurons in the Visual task

We carried out 258 penetrations (173 in M1 e 85 in M2) in the left hemispheres of the LPFC of the two monkeys.

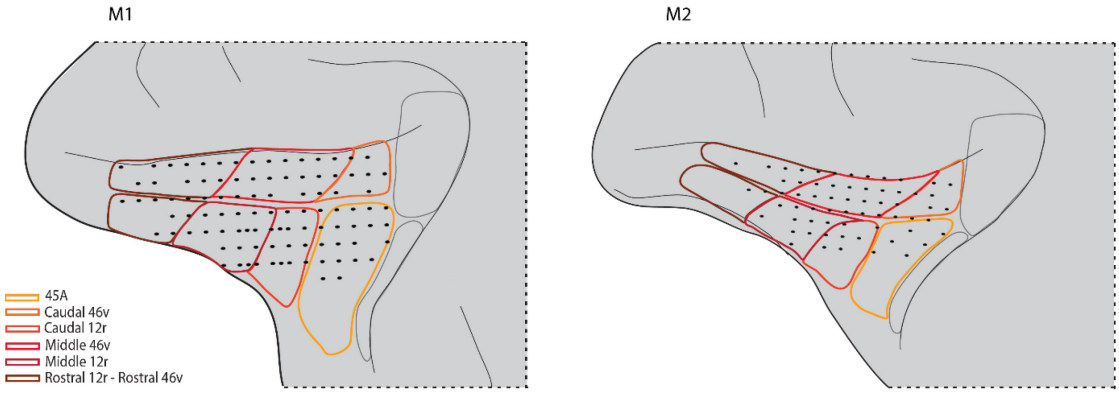

Fig. 9: 2D maps showing the coordinates of penetrations in which at least one neuron was recorded.

The recorded region of each monkey is shown in Figure 9, which shows that the intermediate VLPF is the most investigated territory in terms of number of penetrations.

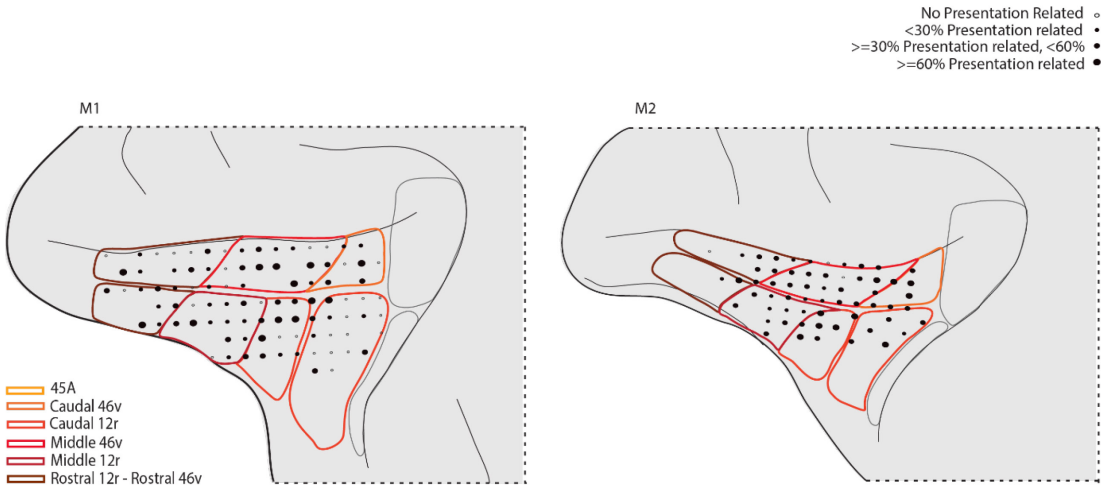

Fig. 10: 2D maps showing the percentage of presentation related neurons with respect to the overall number of recorded neurons in each site. Empty circles represent penetration sites where no presentation-related neurons were detected; filled circles indicate the penetration sites in which at least one task related neuron was recorded.

The percentage of presentation-related neurons is defined by the size of each filled circle, as indicated in the legend over the figure.

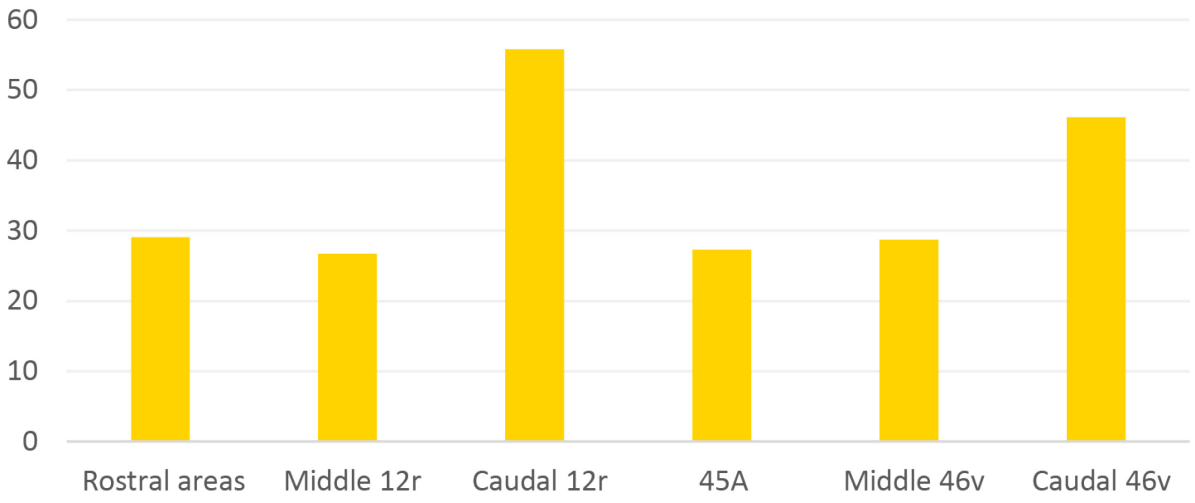

Fig. 11: Histograms depicting the percentage of presentation related neurons with respect to the overall number of recorded neurons in each sector, in both monkeys.

Figure 10 shows the percentage of the presentation-related neurons with respect to the overall number of recorded neurons in each site. In both monkeys, the percentage of presentation-related neurons increases moving to caudal and ventral penetration sites, predominantly involving the caudal portion of area 12r and the adjacent caudal portion of area 46v, while penetration sites located in the other sectors seem to be relatively less involved. The results depicted in Figure 11 confirm this trend, showing that the overall percentage of presentation related neurons with respect to the total number of neurons recorded in each sector, in both monkeys, is higher in the caudal area 12r (56%) and caudal area 46v (46%), with the other sectors all showing an overall percentage of around 25 to 30% of presentation related neurons in this task.

3.2. Distribution of the category-selective and non selective neurons in the Visual task

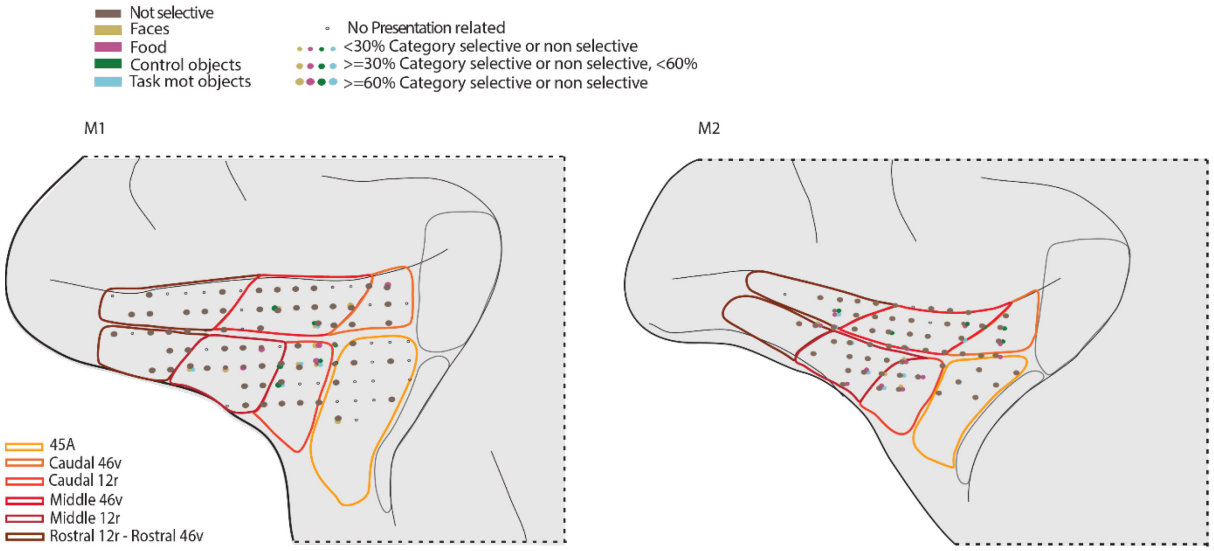

Fig. 12: 2D maps showing the percentage of category selective and non-selective neurons with respect to the presentation related neurons identified in each penetration site. Other conventions as in figure 10.

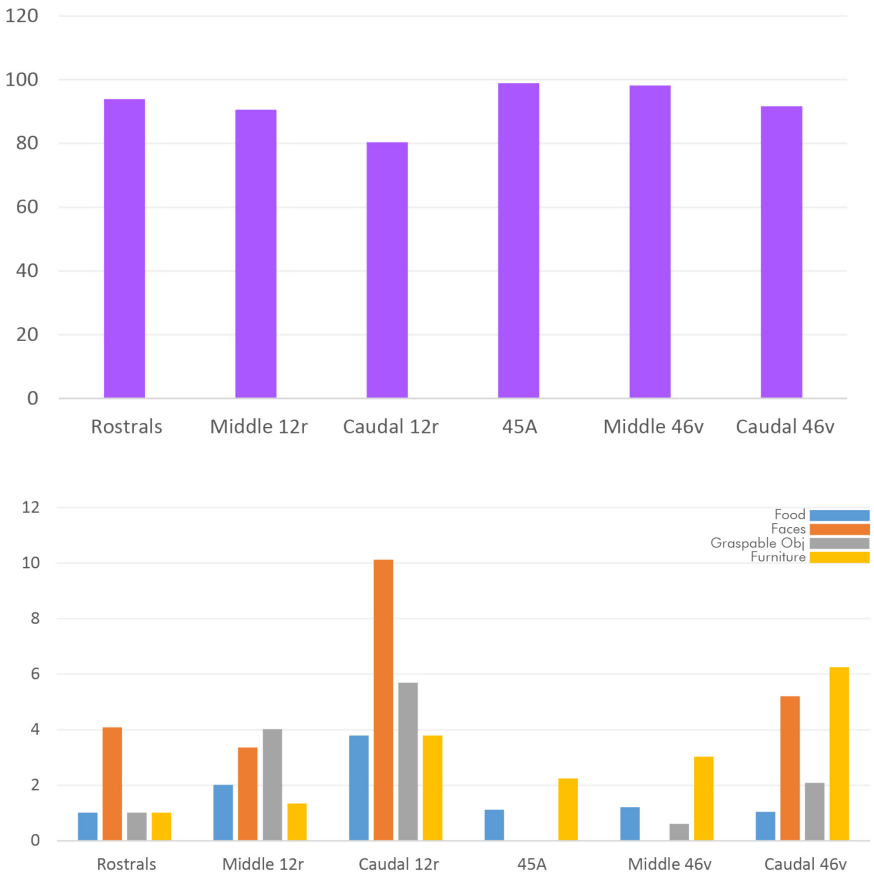

Fig. 13: Histograms depicting the percentage of non-selective (upper part) and category selective (lower part) with respect to the overall number of presentation related neurons in each sector, in both monkeys.

The distribution of category-selective and non-selective neurons in the different penetration sites of the two recorded monkeys is shown in Figure 12. It is possible to observe that in both monkeys the distribution of non-selective neurons is quite homogeneous among the various recorded areas. Regarding the category-selective neurons, on the other hand, it can be seen that they are mainly prevalent at the level of area 12r, particularly in the caudal but also in the intermediate portion of it, and in the caudal portion of area 46v. These results are in line with what is shown in the histograms presented in Figure 13, which represents, respectively, the percentages of non-selective (in the upper part of the figure) and category-selective (lower part) neurons compared to the total number of neurons recorded in each of the considered areas and in both monkeys. It is possible to see that the percentages of non-selective neurons are at the lowest levels (around 80 percent) in caudal and intermediate area 12r and caudal area 46v, while the percentages are quite higher (90-100 percent) in the other areas. Consistent with this, the caudal and middle sector of area 12r and the caudal area 46v show the highest percentages of selective neurons for the category, with the caudal sector of 12r appearing to be mainly characterized by the presence of face selective neurons (10 percent), the middle sector of 12r having similar percentage of face selective and graspable object selective (around 5 percent), while the caudal area 46v having similar percentage of face and furniture selective neurons (around 5-6%).

3.3. Functional properties of neurons recorded in each area in the Visual and Visuomotor tasks

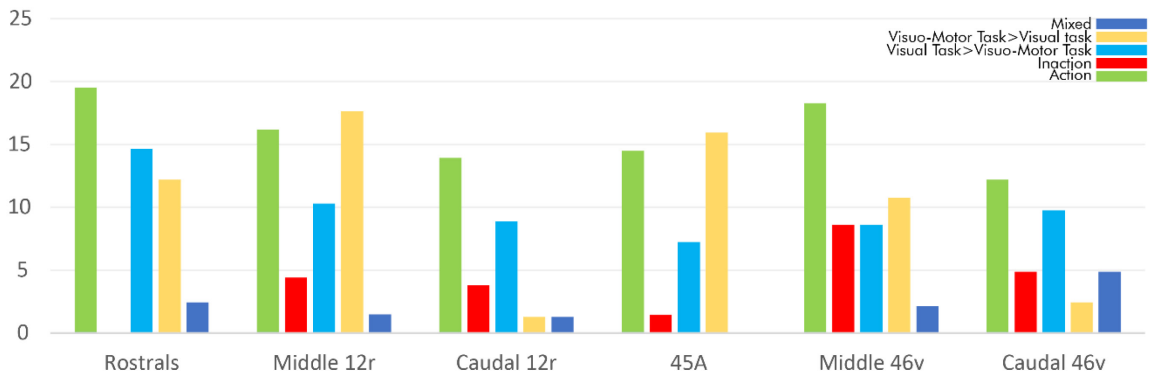

Fig. 14: Histograms depicting, for each area, the percentage of neurons recorded in the Presentation epoch during both the visual and visuomotor tasks showing a preference for the Action (Green) or Inaction (Red) conditions of the Visuomotor task,

the Visuomotor task as a whole (Yellow), the Visual task (Light blue) or having mixed preferences (Dark blue), with respect to the total number of task related neurons recorded in at least one of the tasks.

Figure 14 depicts the percentage of neurons recorded in the Presentation epoch during both the visual and visuomotor tasks showing a selectivity for one of the two conditions of the visuo-motor task, for both conditions of the visuo-motor task over the visual task, for the visual task over both conditions of the visuo-motor task or showing mixed preferences across these tasks. It is possible to see that, overall, the Action condition of the visuo-motor task seems to be the most represented one in all areas, with the rostral areas (20%), area middle 46v (18%) and area middle 12r (16%) showing the highest percentages of these types of neurons. The second most represented category is the one preferring the Visuo-Motor task over the Visual task, as visible in area Middle 12r (18%) and in area 45A (16%). Finally, neurons preferring the Visual task over the Visuo-motor one are represented relatively equally in all the considered areas, with percentages around 8%-10%, with the exception of the Rostral areas, amounting to 15%. The mixed category is the least represented one, amounting to 5% or below in each considered area.

3.4. dPCA of the activity recorded during the Visual task

A demixed Principal Component Analysis (dPCA, see Methods) was performed on the population of presentation-related neurons of each anatomical subdivision, to evaluate how the population of each of these subdivisions encodes the different categories of stimuli presented in the Visual task, during the Presentation epoch.

Caudal area 46v

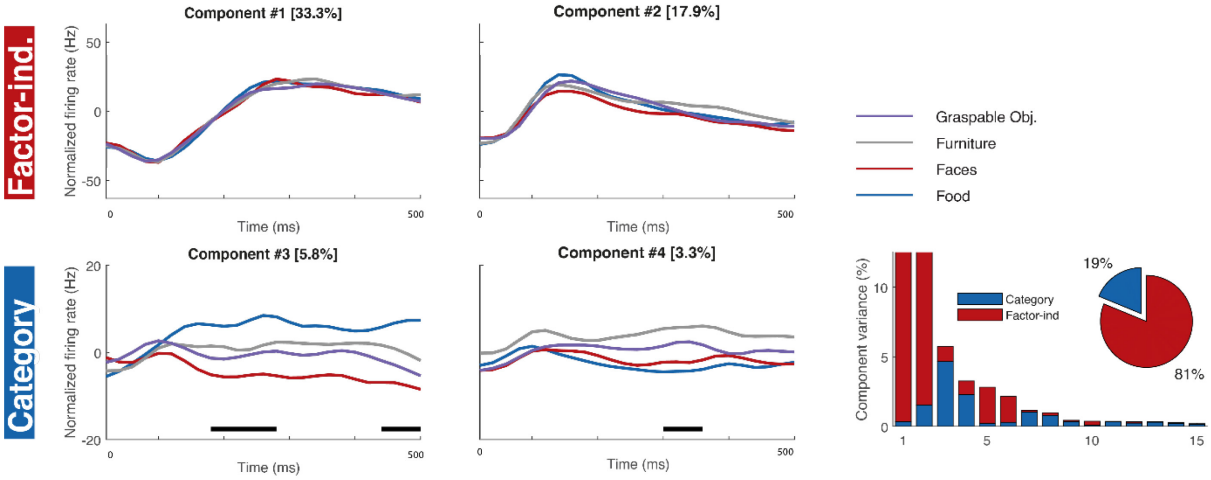

Figure 15: dPCA of the caudal 46v presentation-related neurons recorded during the Presentation epoch of the Visual task. The histograms in the bottom right part of the figure show how much of the percentage of variance explained by the first 15 components identified is factor-independent or attributable to the various task factors. Each panel depicts the time course of the projections of the two largest demixed principal components that can be attributed to the Factor-independent and Category factors for which a significant effect has been observed (see Methods). The purple lines represent the activity recorded in the "Graspable Object" trials, the gray lines represent the activity recorded in the "Furniture" trials, the red lines represent the activity recorded in the "Faces" trials while the blue lines represented the activity recorded in the "Food" trials. Horizontal thick lines indicate the time intervals where the task factor (Category) reliably decoded (see Methods).

Figure 15 shows that in the caudal 46v sector, the majority of the explained variance is factor-independent (81%). The trajectories represented on the first factor-indepedent dPC (Component 1), show a gradual light deflection, occurring just after stimulus presentation and followed by an increase at around 100 ms after the start of the epoch, reaching a plateau until the end of the Presentation epoch. The second factor-independent dPC (Component 2) is instead characterized by a peak around 130-40 ms after stimulus presentation. It is also possible to observe that in this sector, the trajectories associated to the four categories, represented onto the Category-dependent principal components, are significantly different from each other. In the first of these dPCs (Component 3), the difference occurs around 200 ms and approximately 450 ms after stimulus presentation, while in the second Category-related dPC (Component 4), a significant difference is observed around 300-350 ms. This significance seems to be primarily due to a separation of the trajectories representing face and food categories, at least in the first category-related dPCs.

Area 45A

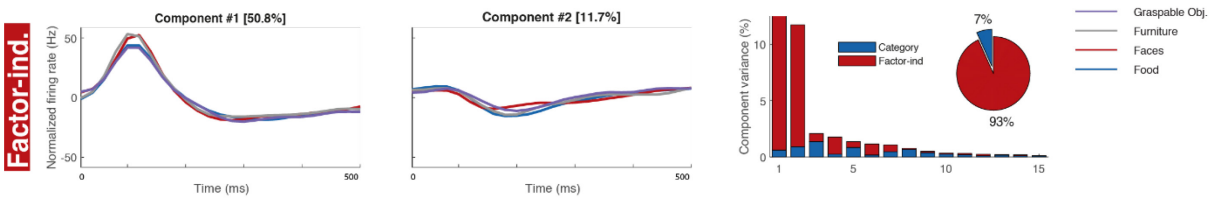

Figure 16: Demixed principal component analysis of the caudal 46v presentation-related neurons recorded during the Presentation epoch of the Visual task. Other conventions as in figure 15.

Figure 16 also indicates that in area 45A the majority of the observed variance, 93%, is explained by the independent factor, while the category accounts for only 7%. Trajectories of the first principal component, independent of the category factor, show a rise in firing rate starting around 50 ms after stimulus presentation, peaking around 100-110 ms, while trajectories of the second component exhibit a slight deviation in firing rate, returning to baseline around 300 ms. Category-related components are absent as no significant differences emerge among trajectories representing the four considered categories.

Caudal area 12r

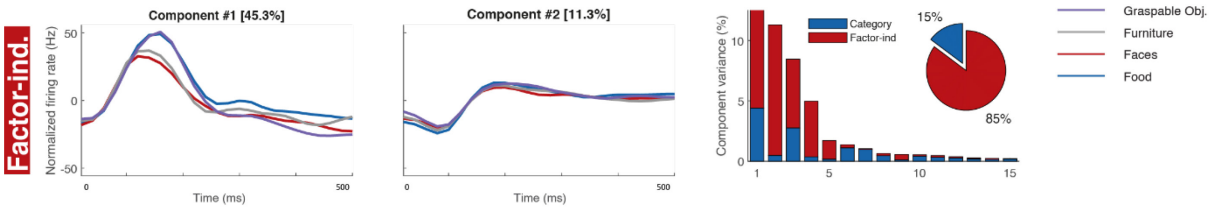

Figure 17: Demixed principal component analysis of the caudal 46v presentation-related neurons recorded during the Presentation epoch of the Visual task. Other conventions as in figure 17.

Figure 17 shows that the majority of the variance, 83%, is explained by the independent factor, while the category explains 15%. Trajectories of the first factor-independent principal component exhibit a rising rate around 50 ms, peaking around 160 ms, especially for object and face components, followed by a gradual decrease. The second component shows a slight decline around 100 ms, followed by an upward trend whose peakis reached around 170 ms, followed by a stabilization/plateau. Note that this component should mostly represent effects that are that are not related to the

Category factor, but it is still capturing Category-related variance, as it is possible to observe in the histograms shown on the right part of the figure. This could explain the category-related modulation that is observed in component #1.

Middle area 12r

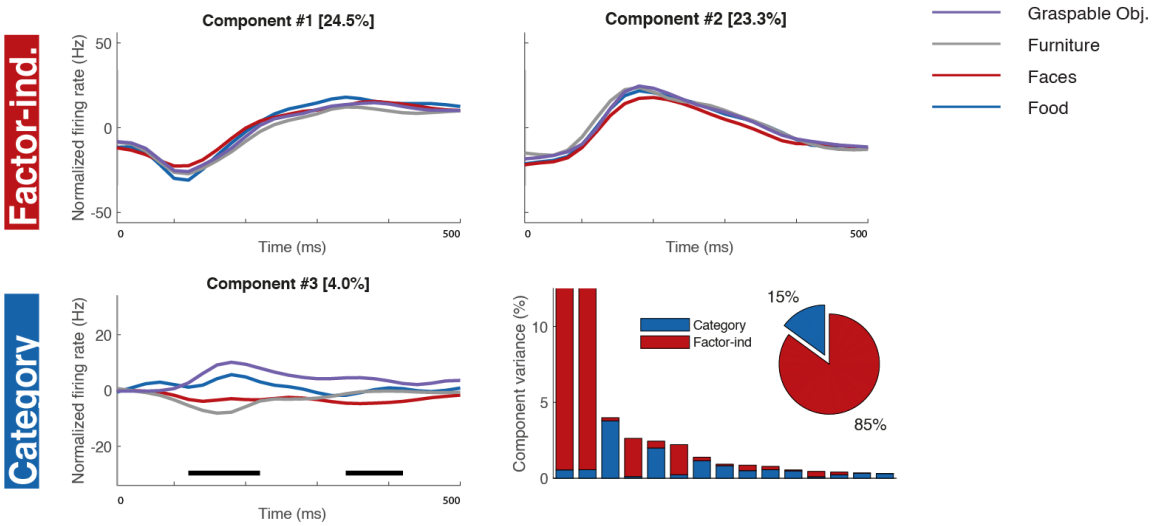

Figure 18: Demixed principal component analysis of the middle 12r presentation-related neurons recorded during the Presentation epoch of the Visual task. Other conventions as in figure 15.

Figure 18 once more reveals that the majority of the variance (85%) is factor-independent, while the factor Category accounts for 15% of the variance. The first component of the independent factor shows a slight valley around 100 ms, with a gradual but limited increase in firing rate reaching a plateau around 300 ms after stimulus presentation. Trajectories of the second component of the independent factor show a gradual increase starting around 100 ms, then going back to the epoch average levels around 400 ms. Considering the first Category-related component, significant distinctions are observed in trajectories around 150-250 ms, potentially influenced by all stimulus types (Component 3). Notably, a dyadic trend is observed, with Graspable objects and Food showing increased activity and Furniture and Faces remaining stable (in the case of Faces) or exhibiting slight deflection (Furniture).

Middle area 46v

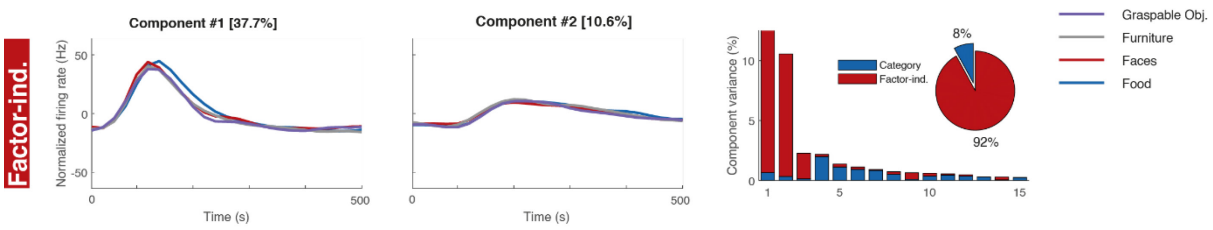

Figure 19: Demixed principal component analysis of the caudal 46v presentation-related neurons recorded during the Presentation epoch of the Visual task. Other conventions as in figure 15.

Figure 19 shows that the majority of the variance, 92%, is Factor-independent, while only 8% is explained by the Category factor. In the first component of the independent factor, a gradual increase in firing rate begins around 50 ms, peaking around 130-140 ms, and then decreases, reaching a stable value around 250 ms. During the peak, a slight deviation is observed in the food category, whose response appears slightly delayed compared to other stimulus types. Conversely, the second component exhibits a much more gradual and prolonged increase in firing rate, starting around 150 ms, peaking around 190 ms, and then gradually declining, returning to baseline levels near 500 ms.

Rostral areas 46v-12r

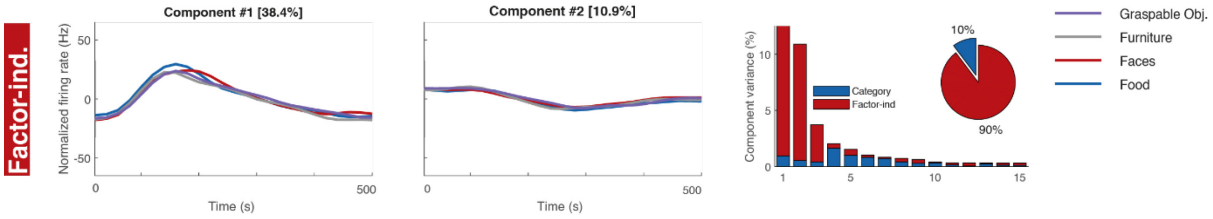

Figure 20: Demixed principal component analysis of the caudal 46v presentation-related neurons recorded during the Presentation epoch of the Visual task. Other conventions as in figure 15.

In Figure 20, it is evident that 90% of the variance is independent of the factor, while only 10% can be attributed to the Category factor. Trajectories in the first independent factor component show a gradual rise starting around 100 ms, peaking around 150 ms, and beginning to gradually descend around 200 ms until the end of the epoch.

3.5. Temporal profile and dPCA of the activity of each area in the Presentation phase of the visuo-motor and visual tasks

In order to evaluate and compare the behaviour and the time course of the activity of the task-related neurons in each area during the Presentation phase of the visuo-motor and visual tasks, we plotted the mean net activity of the neurons of each area aligned with the Presentation epoch, in three conditions: Action and Inaction for the visuo-motor task and Visual for the visual task.

Caudal 46v

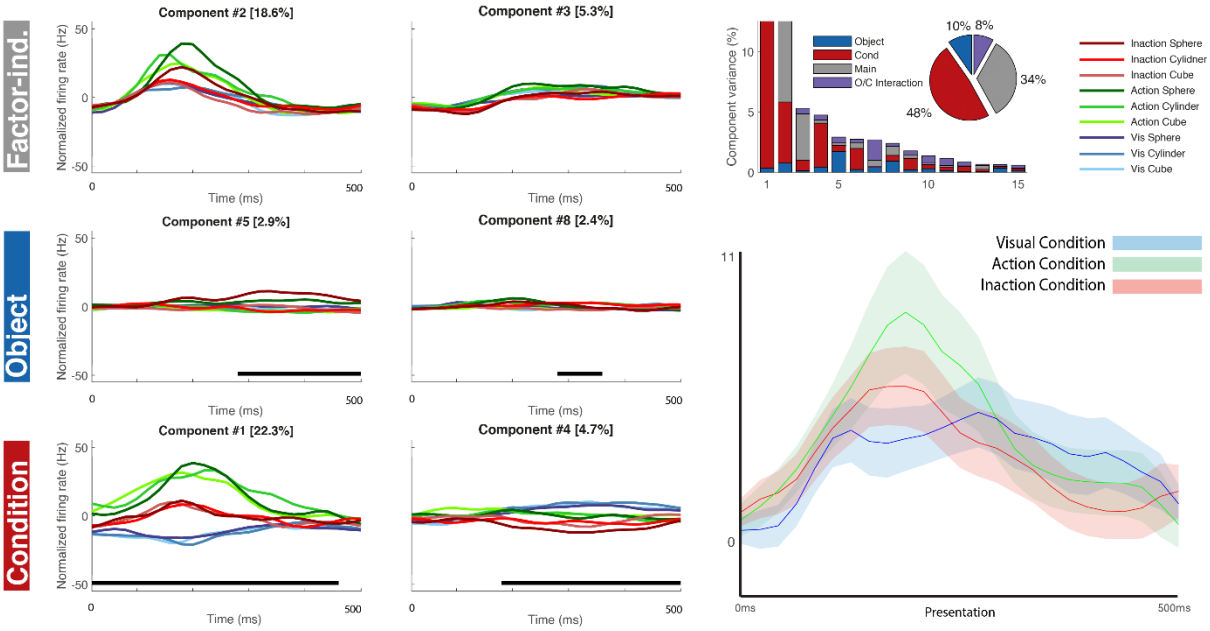

Fig. 21, lower right part: Mean-net neural activity for the three conditions aligned with the Presentation epoch, in the populations of neurons of caudal 46v. The green, red and blue curves indicate the task-related population mean net activity in the Action, Inaction and Visual condition. The shaded area around each curve represents an interval of +-1 standard error around the mean activity observed in each bin of each condition. Fig 21 left part: dPCA of caudal area 46v neurons recorded during the Presentation epoch of the Visual and Visuomotor tasks. The histograms in the upper right part of the figure show how the percentage of variance explained by the first 15 components identified is distributed among the task factors. Each panel depicts the time course of the projections of the two largest demixed principal components that can be attributed to the Factor-independent, Condition or Object factors for which a significant effect has been observed (see Methods).

Figure 21 shows the time course and the intensity of the response of task-related neurons for the three conditions in caudal area 46v, showing that this population of neurons has a peak in response at around 200 ms after stimulus presentation in the Action condition, while the response is lower in the Inaction and

Visual conditions in this same time period. The response then decreases earlier in the Action and Inaction condition, at around 250 ms, while this decrease is delayed in the Visual condition, in which the response is maintained at a relatively stable level until around 400 ms after stimulus presentation. The statistical analysis reveals that the response in the three conditions is not significantly different.

In the left part of figure 15, it is possible to observe that the condition factor explains the majority of variance (48%), the object factor explains 10% of it, while the interaction factor 8% and the remaining 34% is independent by the mentioned factors. The trajectories represented on first factor independent component (Component #2) show a differentiation between the Action condition with respect to the Inaction and the visual ones, in line with the fact that this component, as shown in the histograms depicted in the right part of the figure, is capturing also condition and object related variance.

In the first component dependent on the Condition (Component #1), the trajectories representing the various conditions are significanlty different one from the other during almost the entire epoch. A similar trend, although less evident, was observed in the second component dependent on the Condition (Component #4) starting from 180 ms after stimulus presentation (Fig. 21, lower part). Figure 21 (middle part) shows that the trajectories of the first component dependent on Object (Component #5) are significantly different from around 280 ms to the end of the epoch, while those of the second component (Component #8) significantly separate starting from about 280 ms up to about 360 ms, although in both components the trajectories related to the various objects did not differ according to the type of object. This is in line with the fact that the histograms depicted in the right part of the figure show that these components are also capturing Interaction-related variance.

Caudal 12r

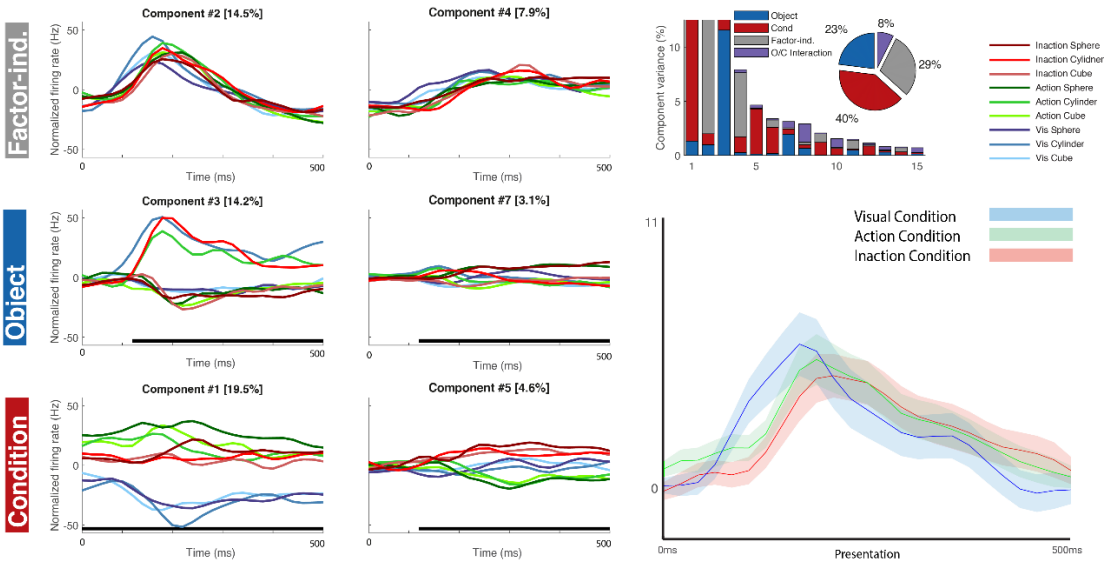

Fig 22: left part: dPCA caudal area 12r neurons recorded during the Presentation epoch of the Visual and Visuomotor tasks. Fig. 22, Right part: Mean-net neural activity for the three conditions aligned with the Presentation epoch, in the populations of neurons of caudal area 12r. The green, red and blue curves indicate the task-related population mean net activity in the Action, Inaction and Visual condition. Other conventions as in fig. 21.

Figure 22, left part shows that most of the variance is explained again by the Condition factor (40%), while the object factor explains 23%, the interaction 8% and the remaining 29% is factor independent. In the first component dependent on the Condition (Component #1), the trajectories of the various conditions are significantly different one from the other almost during the entire epoch; a similar trend, although less evident, was observed in the second component dependent on the Condition (Component #4) starting 120 ms after stimulus presentation. The trajectories of the first and the second component dependent on Object (Component #3 and #7) are significantly different from around 110 ms to the end of the epoch; in particular, Component #3 is characterized by a differentiation between the trajectories representing the cylinder, in all three conditions, and all other trajectories, while Component #7 is characterized by a differentiation of the trajectories representing the cube, mainly in Action and Inaction condition of the visuo-motor task.

Figure 22, lower right part, shows the time course and the intensity of the response of task-related neurons for the three conditions in caudal area 12r. This population of neurons is characterized by a peak of response which is earlier and higher in the Visual condition compared to the Action and Inaction ones. Starting from around 200 ms after

stimulus presentation, it is possible to observe that the response of the population is, instead, very similar across conditions. The statistical analysis reveals that the response in the three conditions is not significantly different.

45A

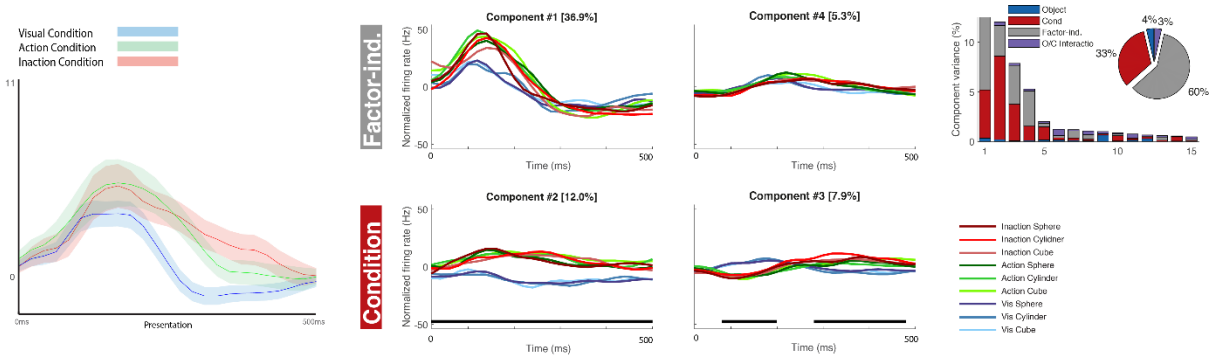

Figure 23: left part: Mean-net neural activity for the three conditions aligned with the Presentation epoch, in the populations of neurons of middle area 45A.
Right part: dPCA of 45A neurons recorded during the Presentation epoch of the Visual and Visuomotor tasks. Other conventions in fig. 21.

Figure 23, left part, shows the time course and the intensity of the response of task-related neurons for the three conditions in area 45A. It is possible to observe that these neurons are characterized by an increase in firing rate occurring around 100 ms after stimulus presentation, reaching a peak at around 200 ms. The response in the Visual condition is, in this epoch, significantly lower than that observed in both Action and Inaction conditions (one-way ANOVA main effect and following post-hoc tests, $p < 0.01$, see Methods). In particular, the discharge rate observed in the Visual condition is already lower than that observed in the other two conditions at the time of the peak and is further characterized by an abrupt decrease around 250 ms from stimulus presentation. The other two conditions, and in particular the Inaction one, are instead associated with a more delayed and gradual decrease of the response following the observed peak.

In Figure 23, right part, the majority of the variance, amounting to 60%, is factor-independent; the factor condition explains 33% of the variance, while object and interaction factors explain 4% and 3% respectively. The upper part of figure 23 shows that, in 45A, the first factor-independent component (Component #1) is characterized

by a differentiation between trajectories associated to the visual and visuomotor tasks. Note that, as previously described, this modulation attributable to the Condition factor, which is present in a factor-independent component, is due to the fact that this component is capturing also part of the Condition-related variance. In the first and in the second component dependent on the Condition (Components #2 and #3), the trajectories of the visual task are significantly different with respect to those of the visuomotor task; in component #2, this difference characterizes the entire epoch, while in the component #3 it is present exclusively around 90-200 ms and 290-490 ms after stimulus presentation. The trajectories of the components dependent on the factor Object did not show any significant difference.

Middle 46v

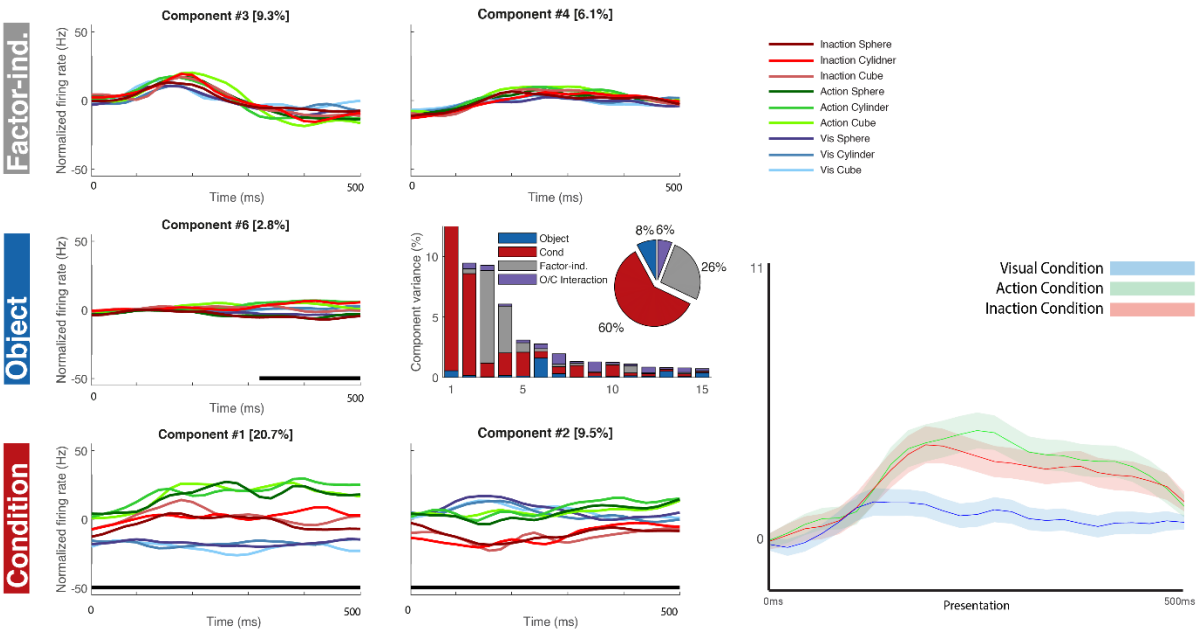

Fig. 24: Left part: Demixed principal component analysis of area Middle 46v neurons recorded during the Presentation epoch of the Visual and Visuomotor tasks.
Right part: Mean-net neural activity for the three conditions aligned with the Presentation epoch, in the populations of neurons of middle area 46v. The green, red and blue curves indicate the task-related population mean net activity in the Action, Inaction and Visual condition. Other conventions as in fig. 21.

Figure 24, right part, shows the time course and the intensity of the response of task-related neurons for the three conditions in area middle area 46v. It is possible to observe that the response in the Action and Inaction condition is significantly higher than that observed in the Visual condition (one-way ANOVA main effect, and following

post-hoc tests, $p < 0.01$, see Methods). In particular, there is a gradual increase in response starting from around 200 ms after stimulus presentation only in the Action and Inaction conditions, while in the Visual the response is always at “reference” level (pre-presentation mean activity). The response in the two conditions of the visuo-motor task is then maintained almost until the end of the epoch. It is evident that the condition factor explains the majority of variance (60%), the object factor explains 8% of it, while the interaction factor explains 6%;the remaining 34% is independent of the mentioned factors.

In Figure 24, right part, in the first component dependent on the Condition (Component #1), the trajectories of the various conditions are significantly different one from theother during almost the entire epoch, while in the second component dependent on the Condition (Component #2), similarly to what observed in the Middle 12r sector, the differentiation is mainly due to the trajectories representing the Inaction condition and is present throughout the epoch.

The middle part of the figure shows that only the trajectories of the first component dependent on Object (Component #6) are significantly different, starting from 320 ms to the end of the epoch, although also in this case the trajectories did not differ according to the particular type of object.

Middle 12r

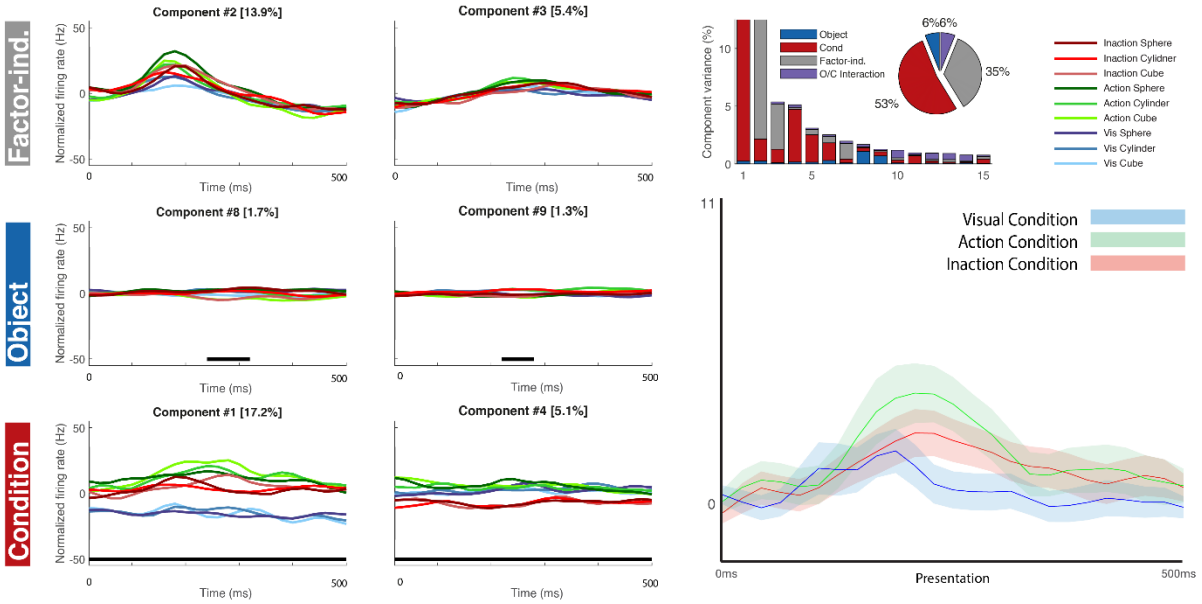

Fig. 25: Left part: dPCA middle area 12r neurons recorded during the Presentation epoch of the Visual and Visuomotor tasks.

Right part: Mean-net neural activity for the three conditions aligned with the Presentation epoch, in the populations of neurons of middle area 12r. The green, red and blue curves indicate the task-related population mean net activity in the Action, Inaction and Visual condition. Other conventions as in fig. 21.

Figure 25, lower right part, shows the time course and the intensity of the response of task-related neurons for the three conditions in middle area 12r. It is possible to observe that, even though statistical analysis did not reveal any significant differences across conditions, this population shows an early and weak rise in its response in the Visual condition, at around 200 ms after stimulus presentation, which is followed by a stabilization of the discharge at the “reference” level, while a stronger and delayed peak, at around 250 ms, occurs during the Action and Inaction condition, with the former showing a stronger response than the latter. The peaked response observed in the Action condition is followed by a relatively abrupt decrease to the “reference” level, while the response observed in the Inaction condition is associated to a more gradual decrease until the end of the epoch.

In Figure 25, left part, most of the variance is explained again by the Condition component (53%), while the object component explains 6%, the interaction component 6% and the remaining 35% is factor independent. In the first component dependent on the Condition (Component #1), the trajectories of the various conditions are significantly different one from the other during almost the entire epoch, in the second

component dependent on the Condition (Component #4) there is a separation between trajectories representing the Inaction condition and those representing the Action and Visual ones, which lasts throughout the epoch. Figure 25 (middle part) shows that the trajectories of the first and the second component dependent on Object (Component #8 and #9) are significantly different for a brief period exclusively around the middle part of the epoch, although in both components the trajectories did not differ according to the type of object.

Rostral areas 12r-46v

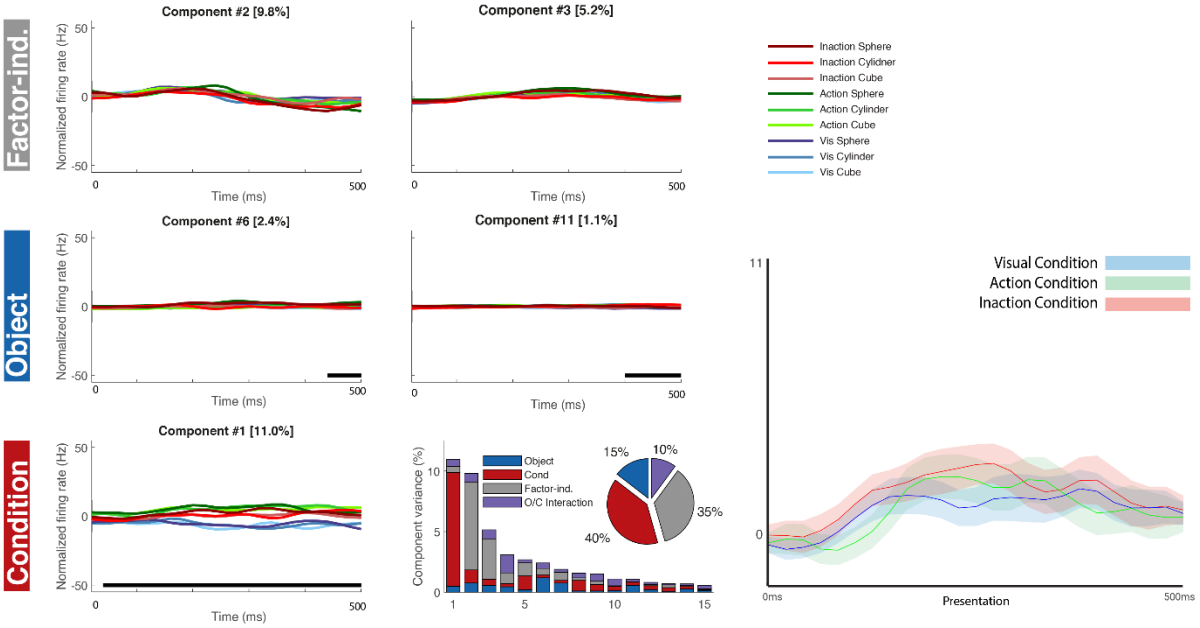

Fig. 26: Left part: Demixed principal component analysis of the Rostral areas 12r-46v neurons recorded during the Presentation epoch of the Visual and Visuomotor tasks.
Right part: Mean-net neural activity for the three conditions aligned with the Presentation epoch, in the populations of neurons of rostral areas. The green, red and blue curves indicate the task-related population mean net activity in the Action, Inaction and Visual condition. Other conventions as in fig. 21.

Figure 26, right part, shows the time course and the intensity of the response of task-related neurons for the three conditions in the rostral areas. This last figure allows to observe that the neurons recorded in the rostral areas which were included in this comparison are very weakly modulated during the presentation epoch in all three conditions, with no significant differences emerging from the statistical analysis. In Figure 26, left part, the condition factor explains the majority of variance (40%), the object factor explains 15% of it while the interaction factor 10% and the remaining 35% is independent by the mentioned factors.

Only in the first component dependent on the Condition (Component #1) there is a significant differentiation, which is due to the trajectories representing the visual condition and lasts almost during the entire epoch (Fig. 32 lower part).
The middle part of this figure shows that the trajectories of the first and the second component dependent on Object (Component #8 and #9) are significantly different for a brief period exclusively around the end of the epoch; although in both components the trajectories related did not differ according to the type of object.

4. Discussion

This study was aimed at verifying whether VLPF areas play a distinct role in processing visual information in different contexts. To this aim, we recorded single neurons activity from two monkeys involved in a passive visual task in which several stimuli were presented and in a visuo-motor task, in which three real objects (also shown as pictures in the passive task) were presented in an Action condition (in which the monkey had to subsequently grasp them) and in an Inaction condition (in which the monkey had to refrain from acting). To this aim, we firstly divided the VLPFC in different sectors, based on their connectivity properties. Subsequently, we analyzed, in each identified hodologic sector, the neuronal responses recorded when the objects were presented in the two aforementioned tasks.

The caudal VLPF areas are more often involved in visual processing than those of the mid-anterior region

Our results show that neural responses to the passive observation of bidimensional stimuli were more frequent in the caudal and middle 12r and caudal 46v, which also hosted the majority of category-specific neurons. In addition, caudal and middle areas 12r are characterized by relatively high percentages of neurons selectively responding to "faces" and "graspable objects", while caudal area 46v mostly presents neurons responding to “faces” and “furniture”.

In line with these results, the dPCA shows that factor-independent modulations are stronger and highly tuned to the presentation of the stimuli in caudal 12r; a similar effect is also observed in area 45A. In addition, the estimated variance attributable to the Category factor is high especially in caudal and middle areas 12r and in the caudal area 46v. It was also observed that these sectors are those characterized by the most interesting differentiations between trajectories representing the different categories, in particular when considering the caudal and middle areas 12r, in which we observed a differentiation that seems to be attributable to "graspable objects" and "food" categories. Since middle 12r is connected to AIP and F5, a working hypothesis is that this differentiation can be related to the presence of neurons similar to the classical visual and visuomotor neurons belonging to the parieto-premotor grasping circuit (Murata et al., 1997, 2000; Raos et al., 2006; Rozzi et al., 2021).

Note that caudal area 12r is actually not characterized by a significant differentiation between the trajectories represented in the category-related components, even though the category factor seems to be actually modulating the neural activity of this sector, as can be seen by the behavior of the trajectories represented in the first factor-independent component as well as by the high percentage of variance explained by the category factor. This apparent contradiction can be explained by the fact that the demixing procedure, which is fundamental in this type of analysis, was not entirely successful, leading to the identification of dPCs which were labeled as “factor-independent” but were actually capturing a relatively high amount of category-related variance. This could explain the fact that a category-related modulation is actually observed in this type of component.
Altogether, these data are in line with the fact that all these sectors, and especially caudal and middle 12r, are target of inferotemporal projections conveying higher order visual information, possibly used by these VLPF regions for memory-based or attentional processes.

The caudal sector of VLPF is involved in visual processing per se, while the intermediate sector is more involved in exploiting visual information for action guidance.

In this thesis, we compared the visual response evoked by the same stimuli in three different experimental conditions: Action, Inaction and Visual. These results showed that almost all sectors, and in particular the middle ones, are characterized by an higher preference for the Action condition, followed by the Visual one. The Inaction condition seems to be preferentially encoded by neurons located in the intermediate and caudal portions of areas 46v and 12r. In addition, the neurons showing a preference for both conditions of the Visuo-motor task (Action and Inaction) over the Visual condition of the Visual task are well represented in all sectors except caudal 12r and caudal 46v.

Caudal area 46v has a role in preparing the oculomotor response following object presentation

Caudal 46v is characterized by the strongest response to stimulus presentation across conditions, when considering mean-net activity, with the Action condition eliciting the strongest response compared to the other two conditions, even though this difference is not statistically significant. This result is confirmed by the dPCA showing that this sector is characterized by a very strong differentiation among all three conditions. This strong modulation, which is mostly attributable to the Action condition, in which, following stimulus presentation, a grasping action has to be performed, along with the strong connections that this sector has with the parietal and frontal areas involved in oculomotor control, could possibly indicate a preparation of the oculomotor response associated to the grasping action to be performed. This interpretation is in line with the notion that the execution of grasping actions occurs in coordination with appropriate eye movements (Caprara & Janssen, 2021; 2022).

Area 45A is involved in processing visual stimuli features, probably based on temporal input.

Neuronal activity recorded in area 45A is characterized by one of the strongest responses to stimulus presentation across the various conditions, as shown by the mean-net activity. On the other hand, dPCA and time course of the population response indicate that this area is characterized by a moderate condition dependent modulation, which is mostly due to a differentiation between the Visual task and the two conditions of the Visuomotor task. A possible hypothesis, grounded on the well-known connections with the inferotemporal cortex (Gerbella et al., 2010), is that this area is involved in the differential encoding of the 3D vs the 2D aspects of the object. An alternative hypothesis is that the difficulty of the task (either deciding to act or refrain from acting vs. simply observing) could modulate neurons of this area. Also this hypothesis has an anatomical plausibility, since area 45A is characterized by rich intra-prefrontal connections. Further, more specific studies are needed to disentangle between these two, not mutually exclusive hypotheses.

Caudal area 12r is involved in coding object identity.

The dPCA of the neuronal activity recorded in caudal 12r shows a relatively strong coding of the type of object, independent of the condition in which it is presented. This result is in line with the fact this sector contains a high number of neurons selectively responding to the presentation of “graspable objects” in the Visual task. Similarly to what observed in area 45A, the dPCA shows that this sector is characterized by a moderate condition dependent modulation. In addition, both dPCA and the plot of the mean-net activity of the neuronal population show that the Visual condition elicits a relatively stronger and earlier activation compared to the Action and Inaction conditions. Thus, it appears that also caudal area 12r is strongly involved in coding visual information about objects, often independent of its behavioral value. This role is in line with a large body of literature indicating that the sector of prefrontal cortex including this area plays a role in the top-down modulation over the temporal cortex, responsible of mnemonic and attentional processes.

Middle area 46v is involved in encoding visual stimuli in terms of the associated behavioral outcome (either action or inaction)

Middle area 46v is the VLPF sector showing the strongest differential coding of the factor condition. The time course of the population activity clearly shows that Action and Inaction conditions elicit a similar discharge profile, stronger than that observed in the Visual condition. Notably, the modulation shown by the trajectories is very weak in the Visual condition. These results are in agreement with the described connectivity pattern of this area with the parieto-premotor grasping circuit (Gerbella et al. 2013) and with the electrophysiological studies showing that this prefrontal sector hosts neurons encoding the behavioral output during the execution or withholding of an action (Rainer et al., 1999; Simone et al. 2015).

Middle area 12r is involved in the pragmatic coding of objects.

Differently from caudal area 12r, in middle area 12r the type of object is very poorly encoded (as shown by dPCA). In contrast, the factor condition is more relevant for the neuronal discharge. This is confirmed also by population analysis showing that

the Action condition elicits the strongest response, followed by the Inaction and Visual ones. These results, together with the selectivity for graspable objects observed in the Visual task and the connectivity with the parietal area AIP, suggests that this sector ise involved in the pragmatic coding of the objects features.

Rostral prefrontal areas seems to be less involved in the functions studied by our task

For technical reasons, only a small number of penetrations were carried out in the rostralmost sector, therefore the number of recorded neurons was not sufficient to functionally separate the distinct anatomical areas falling in the anterior portion of the VLPF. Due to this limitation (see also methods), we decided to consider this anterior portion as a single sector. In addition, neurons in this region appear not to be particularly modulated by the proposed tasks, resulting in a low number of task-related neurons. This is in itself an interesting result, because it evidences the presence of a rather clear functional border between these areas and those posteriorly positioned. As for the population of neurons recorded in the Visual and Visuo-motor tasks, the average response is rather weak and very homogeneous across conditions. This sector is the only one in which both dPCA and the plot of mean population activity do not reveal a particular modulation of the neural activity in one or more conditions. This finding should be interpreted with caution, however, because it may depend on the type of neuronal coding of this region, but also on the fact that the low mean response makes it more difficult for a significant difference to emerge. Thus, the data coming from recording of this sector are too weak to interpret its functional role, but they are certainly sufficiently robust to demonstrate its inhomogeneity with respect to posterior areas, in line with previous connectional and functional studies (Koechlin et al., 2003; Badre & D'Esposito, 2009; Nee & D'esposito, 2016; Riley et al., 2016).

5. Conclusion

The data described in this thesis confirm the idea that the caudal VLPF areas play an important role in the encoding of visual stimuli. In particular, we show that area 45A seems to have a more direct role in the processing of the characteristic of the visual stimuli, without showing particular specificity for the stimulus type or the context in which it is present, while the caudal 12r sector is more involved in coding the object type and could be crucial for perceptual categorization tasks.

Caudal 46v shows interesting transitional features between the posterior and intermediate areas, being strongly responsive to visual stimuli which are already linked to the definition of the behavior to be performed. The intermediate region, overall, seems to be more related to the processing of contextual information for guiding behavior, with a greater involvement of the middle area 46v in encoding the type of task to be performed, differentiating between a task in which an action has to be executed or withheld from a purely passive task, and of the middle area 12r in pragmatic coding of the objects features within the visuo-motor task. Finally, rostral areas are less involved in the aspects investigated by the tasks that were considered in this study.

In conclusion, this study show that prefrontal areas characterized by distinct patterns of cortical and subcortical connectivity also have a specific role in coding contextual visual information.

6. References

Asaad, W. F., Rainer, G., & Miller, E. K. (2000). Task-specific neural activity in the primate prefrontal cortex. *Journal of Neurophysiology*, *84*(1), 451–459. https://doi.org/10.1152/JN.2000.84.1.451

Ashbridge, E., Perrett, D. I., Oram, M. W., & Jellema, T. (2000). Effect of image orientation and size on object recognition: responses of single units in the macaque monkey temporal cortex. *Cognitive Neuropsychology*, *17*(1), 13–34. https://doi.org/10.1080/026432900380463

Averbeck, B. B., Chafee, M. V., Crowe, D. A., & Georgopoulos, A. P. (2002). Parallel processing of serial movements in prefrontal cortex. *Proceedings of the National Academy of Sciences of the United States of America*, *99*(20), 13172–13177. https://doi.org/10.1073/PNAS.162485599/ASSET/34A1CA4F-24B4-4AF2-8975-DD9E5B5CB6D4/ASSETS/GRAPHIC/PQ2024855004.JPEG

Baker, J. T., Patel, G. H., Corbetta, M., & Snyder, L. H. (2006). Distribution of activity across the monkey cerebral cortical surface, thalamus and midbrain during rapid, visually guided saccades. *Cerebral Cortex (New York, N.Y.: 1991)*, *16*(4), 447–459. https://doi.org/10.1093/CERCOR/BHI124

Barbas, H., Saha, S., Rempel-Clower, N., & Ghashghaei, T. (2003). Serial pathways from primate prefrontal cortex to autonomic areas may influence emotional expression. *BMC Neuroscience*, *4*, 25. https://doi.org/10.1186/1471-2202-4-25

Barraclough, N. E., Xiao, D., Baker, C. I., Oram, M. W., & Perrett, D. I. (2005). Integration of visual and auditory information by superior temporal sulcus neurons responsive to the sight of actions. *Journal of Cognitive Neuroscience*, *17*(3), 377–391. https://doi.org/10.1162/0898929053279586

Baumann, M. A., Fluet, M. C., & Scherberger, H. (2009). Context-specific grasp movement representation in the macaque anterior intraparietal area. *The Journal of Neuroscience : The Official Journal of the Society for Neuroscience*, *29*(20), 6436–6448. https://doi.org/10.1523/JNEUROSCI.5479-08.2009

Borra, E., Belmalih, A., Calzavara, R., Gerbella, M., Murata, A., Rozzi, S., & Luppino, G. (2008). Cortical connections of the macaque anterior intraparietal (AIP) area. *Cerebral Cortex (New York, N.Y.: 1991)*, *18*(5), 1094–1111. https://doi.org/10.1093/CERCOR/BHM146

Borra, E., Gerbella, M., Rozzi, S., & Luppino, G. (2011). Anatomical Evidence for the Involvement of the Macaque Ventrolateral Prefrontal Area 12r in Controlling Goal-Directed Actions. *Journal of Neuroscience*, *31*(34), 12351–12363. https://doi.org/10.1523/JNEUROSCI.1745-11.2011

Borra, E., Gerbella, M., Rozzi, S., & Luppino, G. (2015). Projections from caudal ventrolateral prefrontal areas to brainstem preoculomotor structures and to Basal Ganglia and cerebellar oculomotor loops in the macaque. *Cerebral Cortex (New York, N.Y.: 1991)*, *25*(3), 748–764. https://doi.org/10.1093/CERCOR/BHT265

Borra, E., Gerbella, M., Rozzi, S., & Luppino, G. (2017). The macaque lateral grasping network: A neural substrate for generating purposeful hand actions. *Neuroscience and Biobehavioral Reviews*, *75*, 65–90. https://doi.org/10.1016/J.NEUBIOREV.2017.01.017

Borra, E., Gerbella, M., Rozzi, S., Tonelli, S., & Luppino, G. (2014). Projections to the superior colliculus from inferior parietal, ventral premotor, and ventrolateral prefrontal areas involved in controlling goal-directed hand actions in the macaque. *Cerebral Cortex (New York, N.Y.: 1991)*, *24*(4), 1054–1065. https://doi.org/10.1093/CERCOR/BHS392

Borra, E., & Luppino, G. (2021). Comparative anatomy of the macaque and the human frontal oculomotor domain. *Neuroscience and Biobehavioral Reviews*, *126*, 43–56. https://doi.org/10.1016/J.NEUBIOREV.2021.03.013

Bruni, S., Giorgetti, V., Bonini, L., & Fogassi, L. (2015). Processing and Integration of Contextual Information in Monkey Ventrolateral Prefrontal Neurons during Selection and Execution of Goal-Directed Manipulative Actions. *The Journal of Neuroscience*, *35*(34), 11877. https://doi.org/10.1523/JNEUROSCI.1938-15.2015

Carlén, M. (2017). What constitutes the prefrontal cortex? *Science (New York, N.Y.)*, *358*(6362), 478–482. https://doi.org/10.1126/SCIENCE.AAN8868

Caspari, N., Janssens, T., Mantini, D., Vandenberghe, R., & Vanduffel, W. (2015). Covert shifts of spatial attention in the macaque monkey. *The Journal of Neuroscience : The Official Journal of the Society for Neuroscience*, *35*(20), 7695–7714. https://doi.org/10.1523/JNEUROSCI.4383-14.2015

Chafee, M. V., & Goldman-Rakic, P. S. (2000). Inactivation of parietal and prefrontal cortex reveals interdependence of neural activity during memory-guided saccades. *Journal of Neurophysiology*, *83*(3), 1550–1566. https://doi.org/10.1152/JN.2000.83.3.1550

Chandrasekaran, C., Trubanova, A., Stillittano, S., Caplier, A., & Ghazanfar, A. A. (2009). The natural statistics of audiovisual speech. *PLoS Computational Biology*, *5*(7). https://doi.org/10.1371/JOURNAL.PCBI.1000436

Chugani, H. T., Phelps, M. E., & Mazziotta, J. C. (1987). Positron emission tomography study of human brain functional development. *Annals of Neurology*, *22*(4), 487–497. https://doi.org/10.1002/ANA.410220408

Cisek, P., & Kalaska, J. F. (2010). Neural mechanisms for interacting with a world full of action choices. *Annual Review of Neuroscience*, *33*, 269–298. https://doi.org/10.1146/ANNUREV.NEURO.051508.135409

Contini, M., Baccarini, M., Borra, E., Gerbella, M., Rozzi, S., & Luppino, G. (2010). Thalamic projections to the macaque caudal ventrolateral prefrontal areas 45A and 45B. *The European Journal of Neuroscience*, *32*(8), 1337–1353. https://doi.org/10.1111/J.1460-9568.2010.07390.X

Emery, N. J. (2000). The eyes have it: the neuroethology, function and evolution of social gaze. *Neuroscience & Biobehavioral Reviews*, *24*(6), 581–604. https://doi.org/10.1016/S0149-7634(00)00025-7

Ferrari, P. F., Rozzi, S., & Fogassi, L. (2005). Mirror neurons responding to observation of actions made with tools in monkey ventral premotor cortex. *Journal of Cognitive Neuroscience*, *17*(2), 212–226. https://doi.org/10.1162/0898929053124910

Fluet, M. C., Baumann, M. A., & Scherberger, H. (2010). Context-Specific Grasp Movement Representation in Macaque Ventral Premotor Cortex. *Journal of Neuroscience*, *30*(45), 15175–15184. https://doi.org/10.1523/JNEUROSCI.3343-10.2010

Freedman, D. J., Riesenhuber, M., Poggio, T., & Miller, E. K. (2002). Visual categorization and the primate prefrontal cortex: neurophysiology and behavior. *Journal of Neurophysiology*, *88*(2), 929–941. https://doi.org/10.1152/JN.2002.88.2.929

Funahashi, S., Bruce, C. J., & Goldman-Rakic, P. S. (1991). Neuronal activity related to saccadic eye movements in the monkey's dorsolateral prefrontal cortex. *Journal of Neurophysiology*, *65*(6), 1464–1483. https://doi.org/10.1152/JN.1991.65.6.1464

Funahashi, S., Chafee, M. V., & Goldman-Rakic, P. S. (1993). Prefrontal neuronal activity in rhesus monkeys performing a delayed anti-saccade task. *Nature*, *365*(6448), 753–756. https://doi.org/10.1038/365753A0

Funahashi, S., Inoue, M., & Kubota, K. (1993). Delay-related activity in the primate prefrontal cortex during sequential reaching tasks with delay. *Neuroscience Research*, *18*(2), 171–175. https://doi.org/10.1016/0168-0102(93)90019-M

Funahashi, S., & Takeda, K. (2002). Information processes in the primate prefrontal cortex in relation to working memory processes. *Reviews in the Neurosciences*, *13*(4), 313–345. https://doi.org/10.1515/REVNEURO.2002.13.4.313

Gerbella, M., Belmalih, A., Borra, E., Rozzi, S., & Luppino, G. (2007). Multimodal architectonic subdivision of the caudal ventrolateral prefrontal cortex of the macaque monkey. *Brain Structure & Function*, *212*(3–4), 269–301. https://doi.org/10.1007/S00429-007-0158-9

Gerbella, M., Belmalih, A., Borra, E., Rozzi, S., & Luppino, G. (2010). Cortical Connections of the Macaque Caudal Ventrolateral Prefrontal Areas 45A and 45B. *Cerebral Cortex*, *20*(1), 141–168. https://doi.org/10.1093/CERCOR/BHP087

Gerbella, M., Borra, E., Rozzi, S., & Luppino, G. (2016). Connections of the macaque Granular Frontal Opercular (GrFO) area: a possible neural substrate for the contribution of limbic inputs for controlling hand and face/mouth actions. *Brain Structure & Function*, *221*(1), 59–78. https://doi.org/10.1007/S00429-014-0892-8

Gerbella, M., Borra, E., Tonelli, S., Rozzi, S., & Luppino, G. (2013). Connectional Heterogeneity of the Ventral Part of the Macaque Area 46. *Cerebral Cortex*, *23*(4), 967–987. https://doi.org/10.1093/CERCOR/BHS096

Gerbella, M., Rozzi, S., & Rizzolatti, G. (2017). The extended object-grasping network. *Experimental Brain Research*, *235*(10), 2903–2916. https://doi.org/10.1007/S00221-017-5007-3

Ghazanfar, A. A., Nielsen, K., & Logothetis, N. K. (2006). Eye movements of monkey observers viewing vocalizing conspecifics. *Cognition*, *101*(3), 515–529. https://doi.org/10.1016/J.COGNITION.2005.12.007

Goldman-Rakic, P. S. (1987). Development of Cortical Circuitry and Cognitive Function. *Child Development*, *58*(3), 601. https://doi.org/10.2307/1130201

Goldman-Rakic, P. S. (1995). Cellular basis of working memory. *Neuron*, *14*(3), 477–485. https://doi.org/10.1016/0896-6273(95)90304-6

Gray, J. R., Braver, T. S., & Raichle, M. E. (2002). Integration of emotion and cognition in the lateral prefrontal cortex. *Proceedings of the National Academy of Sciences of the United States of America*, *99*(6), 4115–4120. https://doi.org/10.1073/PNAS.062381899/ASSET/39BAA15D-D8D5-4560-889C-5BA2B8E8B090/ASSETS/GRAPHIC/PQ0623818003.JPEG

Hoshi, E., Shima, K., & Tanji, J. (2000). Neuronal activity in the primate prefrontal cortex in the process of motor selection based on two behavioral rules. *Journal of Neurophysiology*, *83*(4), 2355–2373. https://doi.org/10.1152/JN.2000.83.4.2355

Hyvärinen, J. (1981). Regional distribution of functions in parietal association area 7 of the monkey. *Brain Research*, *206*(2), 287–303. https://doi.org/10.1016/0006-8993(81)90533-3

Hyvärinen, J., & Poranen, A. (1974). Function of the parietal associative area 7 as revealed from cellular discharges in alert monkeys. *Brain : A Journal of Neurology*, *97*(4), 673–692. https://doi.org/10.1093/BRAIN/97.1.673

Ibos, G., Duhamel, J. R., & Ben Hamed, S. (2013). A Functional Hierarchy within the Parietofrontal Network in Stimulus Selection and Attention Control. *Journal of Neuroscience*, *33*(19), 8359–8369. https://doi.org/10.1523/JNEUROSCI.4058-12.2013

Koechlin, E., Ody, C., & Kouneiher, F. (2003). The architecture of cognitive control in the human prefrontal cortex. *Science (New York, N.Y.)*, *302*(5648), 1181–1185. https://doi.org/10.1126/SCIENCE.1088545

Levy, R., & Goldman-Rakic, P. S. (2000). Segregation of working memory functions within the dorsolateral prefrontal cortex. *Experimental Brain Research*, *133*(1), 23–32. https://doi.org/10.1007/S002210000397

Lynch, J. C., & Tian, J. R. (2006). Cortico-cortical networks and cortico-subcortical loops for the higher control of eye movements. *Progress in Brain Research*, *151*, 461–501. https://doi.org/10.1016/S0079-6123(05)51015-X

M, P., & DN, P. (1999). Dorsolateral prefrontal cortex: comparative cytoarchitectonic analysis in the human and the macaque brain and corticocortical connection patterns. *The European Journal of Neuroscience*, *11*(3), 1011–1036. https://doi.org/10.1046/J.1460-9568.1999.00518.X

Miller, E. K. (2000). The prefrontal cortex and cognitive control. *Nature Reviews. Neuroscience*, *1*(1), 59–65. https://doi.org/10.1038/35036228

Mistlin, A. J., & Perrett, D. I. (1990). Visual and somatosensory processing in the macaque temporal cortex: the role of “expectation.” *Experimental Brain Research*, *82*(2), 437–450. https://doi.org/10.1007/BF00231263

Mountcastle, V. B., Lynch, J. C., Georgopoulos, A., Sakata, H., & Acuna, C. (1975). Posterior parietal association cortex of the monkey: command functions for operations within extrapersonal space. *Journal of Neurophysiology*, *38*(4), 871–908. https://doi.org/10.1152/JN.1975.38.4.871

Murata, A., Fadiga, L., Fogassi, L., Gallese, V., Raos, V., & Rizzolatti, G. (1997). Object representation in the ventral premotor cortex (area F5) of the monkey. *Journal of Neurophysiology*, *78*(4), 2226–2230. https://doi.org/10.1152/JN.1997.78.4.2226

Murata, A., Gallese, V., Luppino, G., Kaseda, M., & Sakata, H. (2000). Selectivity for the shape, size, and orientation of objects for grasping in neurons of monkey parietal area AIP. *Journal of Neurophysiology*, *83*(5), 2580–2601. https://doi.org/10.1152/JN.2000.83.5.2580

Nee, D. E., & D’Esposito, M. (2016). The hierarchical organization of the lateral prefrontal cortex. *ELife*, *5*(MARCH2016). https://doi.org/10.7554/ELIFE.12112

Nelissen, K., Borra, E., Gerbella, M., Rozzi, S., Luppino, G., Vanduffel, W., Rizzolatti, G., & Orban, G. A. (2011). Action Observation Circuits in the Macaque Monkey Cortex. *Journal of Neuroscience*, *31*(10), 3743–3756. https://doi.org/10.1523/JNEUROSCI.4803-10.2011

Nelissen, K., Luppino, G., Vanduffel, W., Rizzolatti, G., & Orban, G. A. (2005). Observing others: multiple action representation in the frontal lobe. *Science (New York, N.Y.)*, *310*(5746), 332–336. https://doi.org/10.1126/SCIENCE.1115593

Ontogeny and phylogeny. (n.d.). Retrieved March 16, 2024, from https://psycnet.apa.org/record/1979-00001-000

Oram, M. W., & Perrett, D. I. (1994). Responses of anterior superior temporal polysensory (STPa) neurons to “biological motion” stimuli. *Journal of Cognitive Neuroscience*, *6*(2), 99–116. https://doi.org/10.1162/JOCN.1994.6.2.99

Participation of prefrontal neurons in the preparation of visually guided eye movements in the rhesus monkey. (n.d.). Retrieved March 16, 2024, from https://psycnet.apa.org/record/1989-39079-001

Petrides M and Pandya DN. Comparative architectonic analysis of the human and the macaque frontal cortex. In Boller F and Grafman J (Eds)Handbook of Neuropsychology. Amsterdam: Elsevier, 1994: 17e58. (n.d.).

Petrides, M., & Pandya, D. N. (2002). Comparative cytoarchitectonic analysis of the human and the macaque ventrolateral prefrontal cortex and corticocortical connection patterns in the monkey. *The European Journal of Neuroscience*, *16*(2), 291–310. https://doi.org/10.1046/J.1460-9568.2001.02090.X

Petrides, M., Tomaiuolo, F., Yeterian, E. H., & Pandya, D. N. (2012). The prefrontal cortex: comparative architectonic organization in the human and the macaque monkey brains. *Cortex; a Journal Devoted to the Study of the Nervous System and Behavior*, *48*(1), 46–57. https://doi.org/10.1016/J.CORTEX.2011.07.002

Premereur, E., Janssen, P., & Vanduffel, W. (2015). Effector Specificity in Macaque Frontal and Parietal Cortex. *Journal of Neuroscience*, *35*(8), 3446–3459. https://doi.org/10.1523/JNEUROSCI.3710-14.2015

Preuss, T. M., & Goldman-Rakic, P. S. (1989). Connections of the ventral granular frontal cortex of macaques with perisylvian premotor and somatosensory areas: anatomical evidence for somatic representation in primate frontal association cortex. *The Journal of Comparative Neurology*, *282*(2), 293–316. https://doi.org/10.1002/CNE.902820210

Quintana, J., & Fuster, J. M. (1992). Mnemonic and predictive functions of cortical neurons in a memory task. *NeuroReport*, *3*(8), 721–724. https://doi.org/10.1097/00001756-199208000-00018

Riley, M. R., & Constantinidis, C. (2016). Role of prefrontal persistent activity in working memory. *Frontiers in Systems Neuroscience*, *9*(JAN2016). https://doi.org/10.3389/FNSYS.2015.00181/PDF

Rizzolatti, G., Cattaneo, L., Fabbri-Destro, M., & Rozzi, S. (2014). Cortical mechanisms underlying the organization of goal-directed actions and mirror neuron-based action understanding. *Physiological Reviews*, *94*(2), 655–706. https://doi.org/10.1152/PHYSREV.00009.2013

Rizzolatti, G., Fogassi, L., & Gallese, V. (2006). Mirrors of the mind. *Scientific American*, *295*(5), 54–61. https://doi.org/10.1038/SCIENTIFICAMERICAN1106-54

Rizzolatti, G., & Luppino, G. (2001). The cortical motor system. *Neuron*, *31*(6), 889–901. https://doi.org/10.1016/S0896-6273(01)00423-8

Romanski, L. M. (2004). Domain specificity in the primate prefrontal cortex. *Cognitive, Affective & Behavioral Neuroscience*, *4*(4), 421–429. https://doi.org/10.3758/CABN.4.4.421

Romanski, L. M. (2007). Representation and integration of auditory and visual stimuli in the primate ventral lateral prefrontal cortex. *Cerebral Cortex (New York, N.Y.: 1991)*, *17 Suppl 1*(Suppl 1). https://doi.org/10.1093/CERCOR/BHM099

Romanski, L. M., & Averbeck, B. B. (2009). The Primate Cortical Auditory System and Neural Representation of Conspecific Vocalizations. *Annual Review of Neuroscience*, *32*, 315. https://doi.org/10.1146/ANNUREV.NEURO.051508.135431

Saga, Y., Iba, M., Tanji, J., & Hoshi, E. (2011). Development of multidimensional representations of task phases in the lateral prefrontal cortex. *The Journal of Neuroscience : The Official Journal of the Society for Neuroscience*, *31*(29), 10648–10665. https://doi.org/10.1523/JNEUROSCI.0988-11.2011

Saito, N., Mushiake, H., Sakamoto, K., Itoyama, Y., & Tanji, J. (2005). Representation of immediate and final behavioral goals in the monkey prefrontal

cortex during an instructed delay period. *Cerebral Cortex (New York, N.Y.: 1991)*, *15*(10), 1535–1546. https://doi.org/10.1093/CERCOR/BHI032

Sakata, H., Taira, M., Murata, A., & Mine, S. (1995). Neural mechanisms of visual guidance of hand action in the parietal cortex of the monkey. *Cerebral Cortex (New York, N.Y.: 1991)*, *5*(5), 429–438. https://doi.org/10.1093/CERCOR/5.5.429

Saleem, K. S., Miller, B., & Price, J. L. (2014). Subdivisions and connectional networks of the lateral prefrontal cortex in the macaque monkey. *The Journal of Comparative Neurology*, *522*(7), 1641–1690. https://doi.org/10.1002/CNE.23498

Schaffelhofer, S., & Scherberger, H. (2016). Object vision to hand action in macaque parietal, premotor, and motor cortices. *ELife*, *5*(2016JULY). https://doi.org/10.7554/ELIFE.15278

Schultz, W. (2000). Multiple reward signals in the brain. *Nature Reviews Neuroscience 2000 1:3*, *1*(3), 199–207. https://doi.org/10.1038/35044563

Semendeferi, K., Damasio, H. & Van Hoesen, G.W., Soc. Neurosci. Abstr., 20, 587.7, 1994. (n.d.).

Semendeferi, K., Lu, A., Schenker, N., & Damasio, H. (2002). Humans and great apes share a large frontal cortex. *Nature Neuroscience*, *5*(3), 272–276. https://doi.org/10.1038/NN814

Shima, K., Isoda, M., Mushiake, H., & Tanji, J. (2007). Categorization of behavioural sequences in the prefrontal cortex. *Nature*, *445*(7125), 315–318. https://doi.org/10.1038/NATURE05470

Simone, L., Rozzi, S., Bimbi, M., & Fogassi, L. (2015). Movement-related activity during goal-directed hand actions in the monkey ventrolateral prefrontal cortex. *The European Journal of Neuroscience*, *42*(11), 2882–2894. https://doi.org/10.1111/EJN.13040

Smaers, J. B., Rothman, R. S., Hudson, D. R., Balanoff, A. M., Beatty, B., Dechmann, D. K. N., de Vries, D., Dunn, J. C., Fleagle, J. G., Gilbert, C. C., Goswami, A., Iwaniuk, A. N., Jungers, W. L., Kerney, M., Ksepka, D. T., Manger, P. R., Mongle, C. S., Rohlf, F. J., Smith, N. A., … Safi, K. (2021). The evolution of mammalian brain size. *Science Advances*, *7*(18), 9. https://doi.org/10.1126/SCIADV.ABE2101/SUPPL_FILE/ABE2101_SM.PDF

Somel, M., Franz, H., Yan, Z., Lorenc, A., Guo, S., Giger, T., Kelso, J., Nickel, B., Dannemann, M., Bahn, S., Webster, M. J., Weickert, C. S., Lachmann, M., Pääbo, S., & Khaitovich, P. (2009). Transcriptional neoteny in the human brain. *Proceedings of the National Academy of Sciences of the United States of America*, *106*(14), 5743–5748. https://doi.org/10.1073/PNAS.0900544106/SUPPL_FILE/APPENDIX_PDF.PDF

Sowell, E. R., Thompson, P. M., Holmes, C. J., Jernigan, T. L., & Toga, A. W. (1999). In vivo evidence for post-adolescent brain maturation in frontal and striatal regions. *Nature Neuroscience*, *2*(10), 859–861. https://doi.org/10.1038/13154

Sugihara, T., Diltz, M. D., Averbeck, B. B., & Romanski, L. M. (2006). Integration of auditory and visual communication information in the primate ventrolateral prefrontal cortex. *The Journal of Neuroscience : The Official Journal of the Society for Neuroscience*, *26*(43), 11138–11147. https://doi.org/10.1523/JNEUROSCI.3550-06.2006

T, P., A, Z., K, W., DL, C., J, B., JN, G., JL, R., & AC, E. (1999). Structural maturation of neural pathways in children and adolescents: in vivo study. *Science (New York, N.Y.)*, *283*(5409), 1908–1911. https://doi.org/10.1126/SCIENCE.283.5409.1908

Taira, M., Mine, S., Georgopoulos, A. P., Murata, A., & Sakata, H. (1990). Parietal cortex neurons of the monkey related to the visual guidance of hand movement. *Experimental Brain Research*, *83*(1), 29–36. https://doi.org/10.1007/BF00232190/METRICS

Tanji, J., & Hoshi, E. (2001). Behavioral planning in the prefrontal cortex. *Current Opinion in Neurobiology*, *11*(2), 164–170. https://doi.org/10.1016/S0959-4388(00)00192-6

Tanji, J., & Hoshi, E. (2008). Role of the lateral prefrontal cortex in executive behavioral control. *Physiological Reviews*, *88*(1), 37–57. https://doi.org/10.1152/PHYSREV.00014.2007

The frontal lobes and voluntary action. (n.d.). Retrieved March 16, 2024, from https://psycnet.apa.org/record/1994-97376-000

Thompson, K. G., & Bichot, N. P. (2005). A visual salience map in the primate frontal eye field. *Progress in Brain Research*, *147*(SPEC. ISS.), 249–262. https://doi.org/10.1016/S0079-6123(04)47019-8

Tsao, D. Y., & Livingstone, M. S. (2008). Mechanisms of face perception. *Annual Review of Neuroscience*, *31*, 411–437. https://doi.org/10.1146/ANNUREV.NEURO.30.051606.094238

Van Essen, D. C., Donahue, C. J., & Glasser, M. F. (2018). Development and Evolution of Cerebral and Cerebellar Cortex. *Brain, Behavior and Evolution*, *91*(3), 158–169. https://doi.org/10.1159/000489943

Wallis, J. D., Anderson, K. C., & Miller, E. K. (2001). Single neurons in prefrontal cortex encode abstract rules. *Nature*, *411*(6840), 953–956. https://doi.org/10.1038/35082081

Wardak, C., Vanduffel, W., & Orban, G. A. (2010). Searching for a Salient Target Involves Frontal Regions. *Cerebral Cortex*, *20*(10), 2464–2477. https://doi.org/10.1093/CERCOR/BHP315

White, I. M., & Wise, S. P. (1999). Rule-dependent neuronal activity in the prefrontal cortex. *Experimental Brain Research*, *126*(3), 315–335. https://doi.org/10.1007/S002210050740

Wilson, F. A. W., Scalaidhe, S. P. Ó., & Goldman-Rakic, P. S. (1993). Dissociation of object and spatial processing domains in primate prefrontal cortex. *Science (New York, N.Y.)*, *260*(5116), 1955–1958. https://doi.org/10.1126/SCIENCE.8316836

Yamagata, T., Nakayama, Y., Tanji, J., & Hoshi, E. (2012). Distinct Information Representation and Processing for Goal-Directed Behavior in the Dorsolateral and Ventrolateral Prefrontal Cortex and the Dorsal Premotor Cortex. *Journal of Neuroscience*, *32*(37), 12934–12949. https://doi.org/10.1523/JNEUROSCI.2398-12.2012